Institut für Physikalische Elektronik

Institute of Physical Electronics

Universität Stuttgart

Zwei-Jahresbericht 2008

Report 2009

Zwei-Jahresbericht
Report

2008
2009

Redaktion • edited by:

Jürgen H. Werner
Jürgen R. Köhler

Layout:

grafik-service@web.de

Vorwort

Liebe Freunde des *ipe*,

Sie halten hier den Bericht 2008/2009 in Händen. In diesen zwei Jahren hat sich viel am *ipe* und in seinem Umfeld verändert. Während noch im Jahr 2008 die Photovoltaikindustrie geradezu explodiert ist, wurde sie in 2009 von der Wirtschaftskrise erfasst. Dennoch - verglichen mit anderen Industriezweigen - geht es der Photovoltaikindustrie relativ gut. Dem entsprechend finden die Absolventen des *ipe* immer noch ohne Probleme einen guten Arbeitsplatz. Es gibt immer noch viel zu wenige qualifizierte Ingenieure im Bereich der erneuerbaren Energien. Deshalb beteiligt sich das *ipe* am neuen Bachelor-Studiengang „Erneuerbare Energien", der dieses Wintersemester an der Universität Stuttgart begonnen hat. Ab Wintersemester 2010/2011 wird er durch einen Master „Nachhaltige Elektrische Energieversorgung" unserer Fakultät ergänzt werden. In diesem Masterstudiengang bildet die Photovoltaik einen Schwerpunkt.

In der Forschung haben wir unseren Schwerpunkt ganz auf Silizium-basierte Technologien verlagert. So läuft jetzt nicht nur unsere Siebdrucklinie zur Herstellung industrieller Solarzellen, sondern auch die neue Clusteranlage, mit der wir in Zukunft bis zu 30 cm breite Module aus amorphem Silizium herstellen können. Natürlich gehen auch unsere Grundlagenarbeiten weiter.

Ich bedanke mich bei allen Freunden, MitarbeiterInnen und StudentInnen des *ipe* und wünsche Ihnen ein erfolgreiches Jahr 2010!

Stuttgart, Dezember 2009

J. Werner

Jürgen H. Werner

Preface

Dear friends of *ipe*,

You are holding our Report 2008/2009 in your hands. During these two years many things have changed at *ipe* and its surroundings. Whereas in 2008 the photovoltaics industry still exploded, in 2009 the economic crisis caught hold of it. Nevertheless – compared to other industrial branches – the photovoltaics industry is still doing well. Our graduate and PhD students still have no problem in getting an attractive job after leaving *ipe*. There is still a shortage of qualified engineers in the field of renewable energies. This is the reason why *ipe* participates in the Bachelor degree program “Renewable Energies”, which started this winter term at the University of Stuttgart. Our faculty will extend this Bachelor to a Master degree program “Sustainable Electrical Energy Supply”, starting in winter term 2010/2011. The emphasis of this Master degree program is photovoltaics.

Concerning research, we completely shifted our focus to silicon based technologies. For this reason not only our screen printing line is producing industrial solar cells, but also our new cluster tool will be able to produce in future modules of amorphous silicon up to a width of 30 cm.

I would like to thank all friends, the whole staff and the students of *ipe,* and wish you all a successful year 2010!

Stuttgart, December 2009

J. Werner

Jürgen H. Werner


Institut für Physikalische Elektronik

Inhaltsverzeichnis • Table of Contents

Mitarbeiter
People

Dünnschichttechnik

Solarzellen

Mikro - und Optoelektronik

Weltrekord

Institutsleitung • Head of the Institute

Verwaltung • Administration

Gruppe Laserprozesse
Group Laser Processing

(Gruppenleiter / Group Leader: Jürgen Köhler)

Die Gruppe „Laserprozesse” entwickelt neue Technologien zur Laserprozessierung einkristalliner und multikristalliner Silizium-Scheiben. Hierzu zählen die laserunterstützte Abscheidung von Metallkontakten, die Kantenisolierung von Solarzellen sowie die Laser-Dotierung zur Herstellung von ganzflächigen und selektiven Emittern für kristalline Silizium-Solarzellen. Im Vordergrund unserer Arbeiten stehen Grundlagenuntersuchungen zur Laserdotierung von einkristallinem Silizium. Entwicklungsziele sind die Erhöhung des Durchsatzes bei der laserunterstützten Emitterdotierung sowie die Steigerung der Wirkungsgrade von bis zu 156 mm x 156 mm großen einkristallinen und multikristallinen Silizium-Solarzellen auf über 18%.

The “Laser Processing” group explores new technologies for laser processing of mono- and multi-crystalline silicon wafers. Examples are laser assisted metal deposition, laser edge isolation as well as laser doping for full area and selective emitters of crystalline silicon solar cells. The main topic of our research work is the investigation of the fundamental processes involved in pulsed laser doping for the preparation of n^+-doped emitters on mono-crystalline silicon wafers. Development goals are the increase of the throughput rate of the laser doping process as well as the increase of the efficiency of up to 156 mm x 156 mm sized mono- and multi-crystalline silicon solar cells to more than 18%.

Gruppe Technologie
Group Technology

(Gruppenleiterin / Group Leader: Christiane Köhler)

Die Gruppe „Technologie" setzt sich aus den technischen Mitarbeitern des gesamten Instituts zusammen. Damit sind verschiedene Aufgabenstellungen zur Absicherung der Institutsinfrastruktur, zu Prozessen und Prozessschritten sowie zu Routinemesstechniken zusammengefasst. Diese Vernetzung im technischen Bereich ermöglicht eine gute Koordinierung aller anfallenden Arbeiten, sei es bei Routineanalysen, Messplatzerweiterungen, Laborumbaumaßnahmen oder auch bei der Weiterentwicklung wichtiger Technologien, wie Nasschemie, Lithographie, Metallisierung, Diffusion, Oxidation sowie diversen Plasmadepositionsverfahren und vieles andere mehr. Die Techniken sind immer wieder weiterzuentwickeln, verursacht durch neue Anforderungen, die aus den laufenden Projekten erwachsen. Dabei ist die enge Zusammenarbeit bei Planung und Ergebnisdiskussion eine gute Grundlage mit dem Ziel, die Reproduzierbarkeit der Prozesse und Abläufe durch die Entwicklung von Qualitätskontrollstandards und standardisierten Prozessabläufen zu gewährleisten.

The group "Technology" pools all technical assistants and engineers. We support the laboratory infrastructure, perform the different standard processes and do routine measurements. The cross linking of technical experience allows an effective coordination of the requested demands. We make standard analyses, upgrade measurement setups, coordinate the reconstruction of the laboratory and enhance technological processes. We especially work on wet chemistry, metallization, lithography, diffusion and oxidation as well as on different plasma deposition methods etc. All techniques have to be adapted and developed in direction of the requirements of the current scientific projects at *ipe*. Our goal is a high reproducibility of all process steps as described above by developing quality control requirement and standard procedures. A close teamwork on planning and discussion of the results is seen as a proper base.

Gruppe Neue Materialien
Group New Materials

(Gruppenleiter / Group Leader: Gerhard Bilger)

Für die Entwicklung der Solarzellen der dritten Generation leisten neuartige Materialien als passive Beschichtung einen wichtigen Beitrag zur Erzielung gesteigerter Quantenausbeuten mit höchsten Wirkungsgraden. Zudem stellen sie bei der Optimierung von Dotierverfahren für Si-Solarzellen durch Niedertemperatur-Laserprozesse speziell angepasste Prekursoren zur Verfügung. Bei dem hier angewandten Verfahren der Hochfrequenz-Zerstäubung (HF-Sputtern) lassen sich praktisch alle Zusammensetzungen als dünne Schichten herstellen, wobei auch reaktive Gase in weiten Bereichen zugemischt werden können. Für die Charakterisierung dieser Schichten kommen Oberflächen- und Dünnschichtanalysemethoden wie die Sekundärionen-Massenspektrometrie (SIMS) sowie die Röntgen- und Ultraviolett-Photoelektronen-Spektrometrie (XPS, UPS) als unabdingbarer Bestandteil zum Einsatz. Die Oberflächenanalytik unterstützt auch wesentlich alle Forschungs- und Entwicklungsgruppen am *ipe* und wird als Dienstleistungen für andere Institute und die Industrie angeboten.

For the development of third generation solar cells novel materials used as passive coating will contribute significantly to an increased quantum efficiency. Furthermore, the optimization of doping procedures for Si solar cells with low-temperature laser processes requires specifically developed precursors. These materials are processed as thin films by means of high frequency sputtering techniques which admit the preparation of nearly all elemental compositions including reactive gases within wide ranges. For the characterization of these thin films, secondary ion mass spectrometry (SIMS) as well as X-ray and ultraviolet photoelectron spectrometry (XPS, UPS) are used as indispensable analysis methods. The analysis also substantially supports all research and development groups at the *ipe* and is offered to foreign institutes and industry.

Gruppe Dünnschichtsilizium
Group Thin Film Silicon

(Gruppenleiter / Group Leader: Markus Schubert)

Die Arbeitsgruppe „Dünnschichtsilizium” des *ipe* entwickelt Solarzellen und Photodetektoren auf der Basis amorphen und nanokristallinen Siliziums. Flexible Photovoltaikmodule entstehen mit Hilfe der *in-situ* Serienverschaltung. Niedertemperaturprozesse nutzen ultradünne amorphe Siliziumschichten zur Passivierung und Verbesserung kristalliner Siliziumsolarzellen. In der photovoltaischen Systemtechnik vergleichen wir die Standorte Stuttgart, Nikosia und Kairo und untersuchen dabei den Einfluss von Material, Solarzellentyp und Klima auf den Jahresenergieertrag der netzgekoppelten Anlagen. Die dynamische elektronische Verschaltung verbessert die Energieausbeute von Photovoltaiksystemen. Spezielle Dünnschicht-Photodetektoren dienen der schnellen patientennahen Quantifizierung von Herzinfarkt-, Tumor- und Entzündungsmarkern in einem mobilen elektro-optischen Mikrosystem, welches wir in Zusammenarbeit mit mehreren Instituten der Universitäten Tübingen und Stuttgart sowie dem Institut für Mikroelektronik Stuttgart entwickeln.

The “Thin Film Silicon” work group at *ipe* is developing solar cells and photodetectors based on amorphous and nanocrystalline silicon thin films. Flexible photovoltaic modules prove the novel *in-situ* series connection technique. Low temperature processes deposit ultrathin amorphous silicon layers for passivating and improving crystalline silicon solar cells. Photovoltaic system technology compares the locations Stuttgart, Nicosia and Cairo, in order to investigate the effects of different materials, solar cell types, and climates on the annual energy yield of the grid-connected systems. Novel thin film photodetectors enable the quantification of e.g. heart attack, cancer, and inflammation markers in a mobile microsystem for so-called point-of-care testing which we develop in cooperation with several institutes of the Universities Tübingen and Stuttgart, and with the Institut für Mikroelektronik Stuttgart.

Gruppe Industrielle Solarzellen
Group Industrial Solar Cells

(Gruppenleiterin / Group Leader: Renate Zapf-Gottwick)

Die Forschungsaktivitäten unserer Gruppe „Industrielle Solarzellen" zielen auf industrienahe Prozesse, um den Wirkungsgrad von kristallinen Solarzellen zu verbessern. Wir optimieren gezielt an den einzelnen Schritten in der Herstellungskette einer Solarzelle: Verbesserungen am Emitter, am Lichteinfang (an neuen Texturen) und an den elektrischen Kontakten. Der Siebdruck ist eine, vor allem in der Industrie, gebräuchliche Methode, um elektrische Kontakte aufzubringen. Die Kombination aus Sieb, Paste, verschiedenen Druckparametern und der Temperaturen beim Trocknen und Feuern hat großen Einfluss auf den Prozess der Kontaktbildung. Vorderseitenkontaktgitter und vollflächige Metallisierung auf der Rückseite der Solarzelle werden auf geringe optische und elektrische Verluste optimiert.

Our group "Industrial Solar Cells" is engaged in different research activities aiming at higher efficiencies of solar cells in industry oriented processes. Our goal is to improve the different process steps in the production of solar cells: optimizing the emitter, light trapping (new textures) and the electrical contacts. Electrical contacts are fabricated by screen printing, the most commonly used technique in industry. Screen, paste, different print parameters and the temperatures of drying and firing influence the process of contact formation. The contact grid on the front side and the full area back contact are minimized with respect to electrical and optical losses.

Gruppe Charakterisierung
Group Characterization

(Gruppenleiter / Group Leader: Gerda Gläser, Michael Reuter)

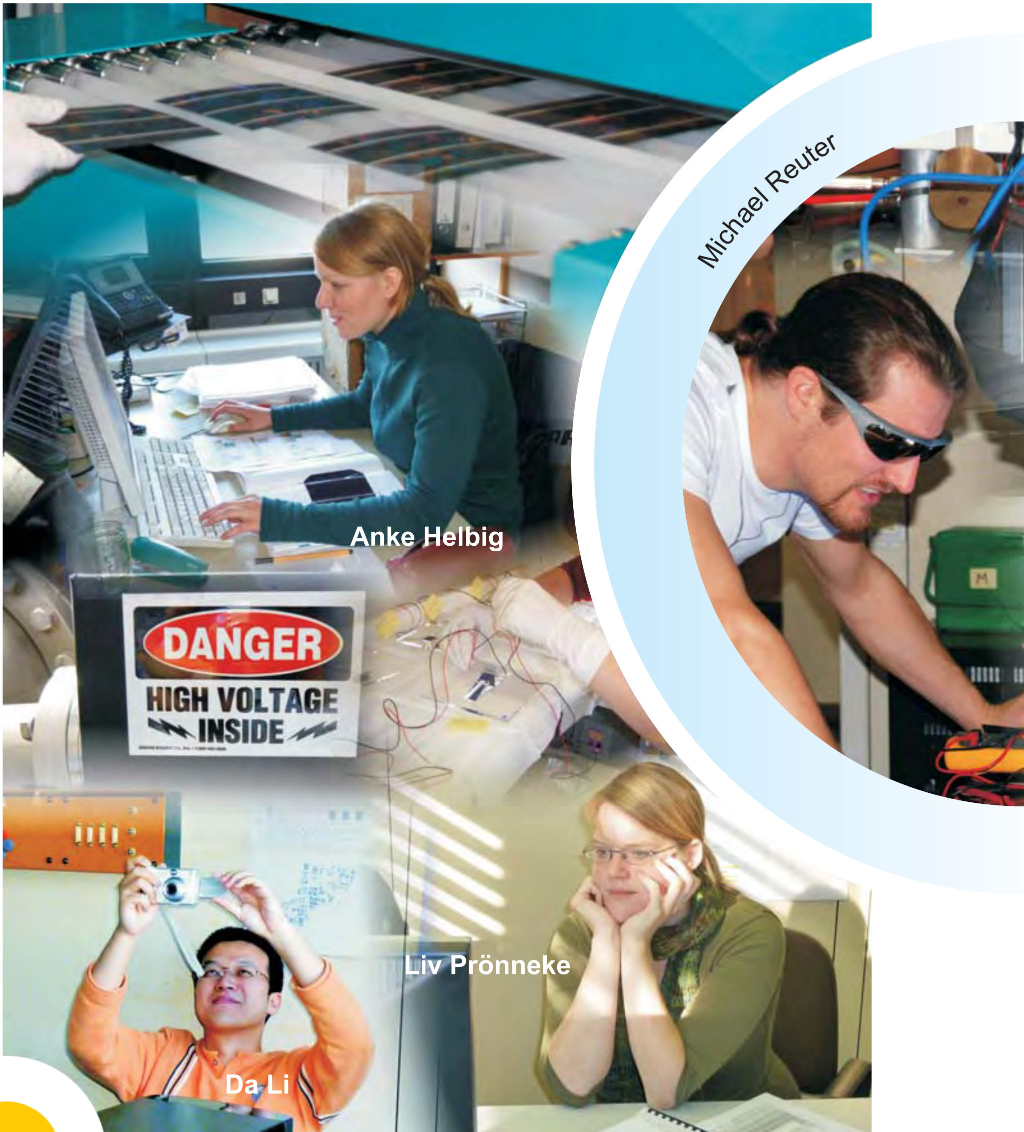

Die Arbeitsgruppe „Charakterisierung" beschäftigt sich mit der Simulation und Analyse von halbleitenden Schichten, Solarzellen und photovoltaischen Systemen. Dabei stehen der Gruppe Aufbauten zur elektrischen und optischen Messung der Lebensdauer, Strom-Spannungscharakteristik, Quantenausbeute, Elektro- und Photolumineszenz und ortsaufgelösten Kurzschlussstromdichte zur Verfügung. Ein weiterer Schwerpunkt ist die Entwicklung von innovativen Konzepten zur Wirkungsgradsteigerung von Solarzellen und -modulen. Optisch aktive Systeme wie Fluoreszenzkollektoren und Filter nutzen dabei konzentrierende bzw. lichtselektive Eigenschaften. Streuzentren in bisher nur elektrisch aktiven Kontakten und Kontaktschichten zielen auf die bessere Einkopplung des Lichts in Solarzellen und Modulen.

The "Device Analysis" group deals with the simulation and characterization of semiconductor layers, solar cells and photovoltaic systems. Thereby, the group makes use of measurements setups for the electrical and optical device characterization, e.g. lifetime measurements, current-voltage characteristics, quantum efficiency, electro- and photoluminescence and spatially resolved short circuit current density measurements. Another focus is the development of novel concepts for the enhancement of photovoltaic efficiency. Optically active systems as fluorescence collectors and filters employ their concentrating and light selective properties to improve the light conversion in solar cells. Scattering of light with so far only electrically active contacts and contact layers aims at the more efficient coupling of light into photovoltaic devices.

einkristallines

mikrokristallines

Silizium

nanokristallines

amorphes

Wissenschaftliche Beiträge
Scientific Contributions

Publikationen
Publications

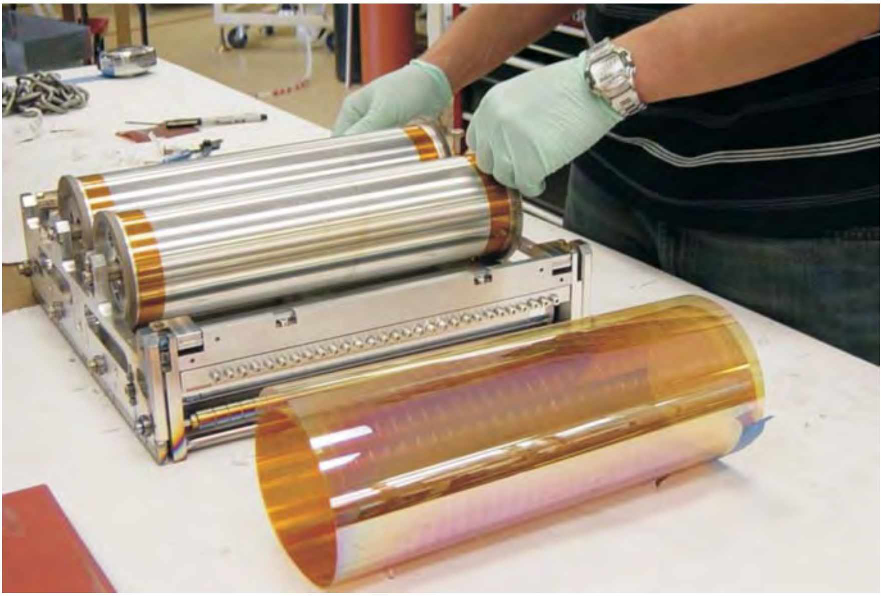

Metal Assisted Texturization for Silicon Solar Cells

Author: J. Cichoszewski
In collaboration with: M. Lipiński and R. Zapf-Gottwick*

Reduction of optical losses by surface texturization is one of the most important fabrication steps of multi-crystalline silicon (mc-Si) solar cells. Unfortunately, anisotropic alkaline texturization is not effective for mc-Si: Each grain receives a different surface texture, depending on its crystallographic orientation. An isotropic texturization, e.g. based on a HF/HNO_3 etching solution, suits better for mc-Si. Nevertheless, isotextured mc-Si solar cells still suffer from high optical losses due to surface reflection.

This work presents a novel texturization method for mc-Si surfaces, which allows for high reduced surface reflection: The metal-assisted chemical etching (MAE). It bases on the deposition of palladium nano-particles from $PdCl_2$ solution as a catalyst for chemical etching in a solution containing HF as acid and HNO_3 as an oxidizing specie [1].

Figure 1a displays the effect of MAE texturization on the reflectivity of finished solar cells with SiN_x antireflective layer and metal front grid. The MAE texture reduces the effective reflectance – integrated over AM1.5 solar spectra over the wavelength regime $400 \leq \lambda \leq 1000$ nm – to R_{eff} = 5.6 %. This value means a 38 % decrease in reflectivity compared to state-of-the-art acidic texturization with R_{eff} = 9 %. In fact, the reflectivity of MAE textured cell gets in the range of KOH textured mono-Si cell with R_{eff} = 3.7 %. A PC1D simulation of a cell with MAE texturization promises an increase of the short circuit current ΔJ_{sc} = + 1.5 mA/cm^2 and an efficiency gain $\Delta\eta$ = + 0.6 % in reference to acidic texture.

Table I presents basic electrical parameters for industrial 15.6 x 15.6 cm^2 mc-Si solar cells with MAE texturization and reference acidic texture. Despite the reduced reflectivity of the cell with the MAE texture, the

*Institute of Metallurgy and Materials Science in Krakow, Polish Academy of Sciences efficiency η of the best MAE textured cell is $\Delta\eta$ = 0.7 % lower than the one with acidic texture, mainly due to a lower value of the short circuit current J_{sc}.

Table I: Best and average electrical parameters for solar cells with MAE and acidic texturization. The average parameters are calculated for five cells of each kind.

Texture		J_{sc} (mA/cm^2)	V_{oc} (mV)	*FF* (%)	η (%)
MAE	best	31.9	615	76.2	14.9
	average	31.4	611	76.4	14.6
Acidic	best	32.7	618	77.3	15.6
	average	32.7	617	76.9	15.5

Figure 1b shows a reduced internal quantum efficiency IQE for a MAE textured cell in the short wavelength region, which hints at a high front surface and a high emitter recombination. We believe, that an optimized emitter MAE texture can strongly improve the performance of mc-Si cell.

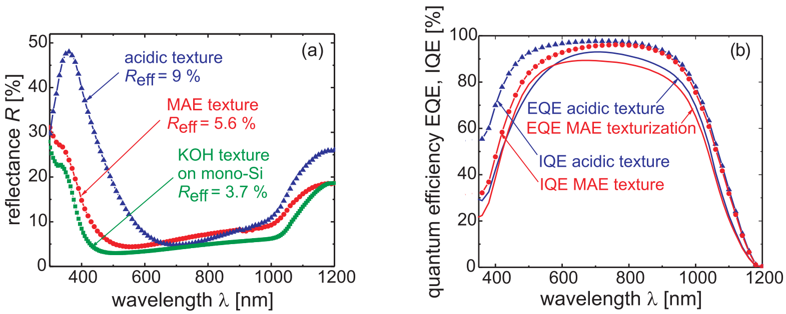

Figure:
a) Reflectivity spectra of ready mc-Si solar cells with SiN_x and front grid contact with MAE and acidic texturization in comparison with the reflectivity of a KOH monocrystalline Si texturization. b) External Quantum Efficiency EQE and Internal Quantum Efficiency IQE of solar cells with MAE texture compared with acidic textured cells. IQE for MAE textured cell is reduced in the short wavelength region.

References:

[1] M. Lipiński, J. Cichoszewski, in *Proc. 23rd Europ. Photovolt. Solar. En. Conf.* (eds. D. Lincot, H. Ossenbrink, and P. Helm, WIP-Renewable Energies, Munich, Germany, 2008) p. 1911.

Thermal Stability of a-SiC:H Passivation Layers

Author: C. Ehling
In collaboration with: M. B. Schubert

Amorphous hydrogenated silicon carbide (a-SiC:H) is a promising material for the photovoltaic industry. When compared with silicon nitride (a-SiN:H), a-SiC:H provides excellent electronic surface passivation on highly doped n^+-type emitters as well as on p^+-type emitters. Moreover, a-SiC:H exhibits a high stability against thermal annealing. Yet, the mechanisms of the electronic surface passivation as well as the structural changes during annealing and firing steps are not well understood. All a-SiC:H layers in this study are grown from Plasma Enhanced Chemical Vapor Deposition (PECVD) of silane (Φ_{SiH4}) and methane (Φ_{CH4}) gas flows on *p*-type monocrystalline silicon (c-Si) wafers. With constant Φ_{SiH4} = 5 sccm, variable Φ_{CH4} changes the gas flow ratio $y = \Phi_{CH4}/(\Phi_{CH4}+\Phi_{SiH4})$, and hence produces films with varying carbon content and layer properties [1].

Figure 1 presents the effective minority carrier lifetime τ_{eff} as a function of sequential annealing in forming gas at various annealing temperatures T_{an}. The T_{an} = 160 °C data represent as-deposited samples. With increasing T_{an}, the τ_{eff} significantly rise for all gas flow ratios *y*. Up to a *y*-dependent maximum, a sufficient flow of atomic hydrogen occurs towards the a-SiC:H/c-Si interface for improving the electronic passivation.

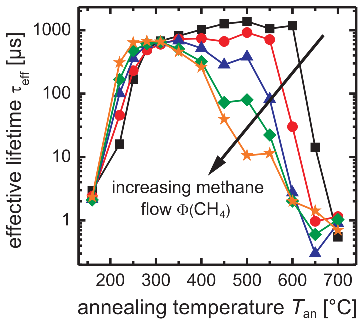

Figure 1:
The effective charge carrier lifetime τ_{eff} and its thermal stability strongly depend on the gas flow ratio *y*. The smallest CH_4 flow yields better thermal stability with τ_{eff} > 1 ms for T_{an} = 600 °C. Enhanced CH_4 flow boosts τ_{eff} at low annealing temperatures T_{an}, but results in less stable passivation towards higher T_{an}.

Around T_{an} = 300 °C, an inflection point divides thermally stable passivation layers for low y from less stable a-SiC:H for high y. The most stable passivation layer yields τ_{eff} > 1 ms up to T_{an} = 600 °C for y = 0.33.

Figure 2 analyzes structural changes of the a-SiC:H films as evident from infrared absorption. The SiH stretching modes at υ = 2000 cm^{-1} represent thermally stable monohydride bonds, while SiH_2 stretching modes at υ = 2080 cm^{-1} indicate void-related dihydride configurations [2]. The absorption spectra remain almost unchanged up to T_{an} = 400 °C, but for higher T_{an} the SiH_2 mode starts shifting from υ = 2080 cm^{-1} to υ = 2065 cm^{-1}, with almost no change of the SiH mode.

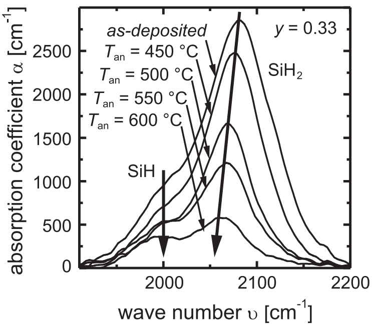

Figure 2:
Absorption spectra of SiH and SiH_2 stretching modes at wave numbers υ = 2000 cm^{-1} and υ = 2080 cm^{-1}, exemplary for the lowest gas flow ratio y = 0.33. At higher annealing temperatures T_{an} ≥450 °C, both peaks decrease in peak height and shift to lower wave numbers, reflecting changes of the Si-H bonding configurations. While isolated SiH bonds prove thermally stable, the SiH_2 mode shifts from υ = 2080 cm^{-1} at T_{an} < 450 °C to υ = 2065 cm^{-1} at T_{an} ≥600 °C.

We conclude that the out-diffusion of hydrogen from voids causes the observed peak shifts. The isolated SiH stretching mode at υ = 2000 cm^{-1} exhibits a higher thermal stability than the void-related contribution at υ = 2065-2080 cm^{-1}. Especially, hydrogen bonds at the interface between the silicon wafer and the passivation layer are considered responsible for the quality and the stability of the electronic passivation.υ = 2080 cm^{-1} to υ = 2065 cm^{-1}, with almost no change of the SiH mode.

References:

[1] I. Solomon, M. P. Schmidt, and H. Tran-Quoc, Phys. Rev. B **38**, 9895 (1988)

[2] G. Lucovsky, R. J. Nemanich, and J. C. Knights, Phys. Rev. B **19**, 2064 (1979)

Sputtered Phosphorus Precursors for Homogeneous Laser Doping

Author: S. J. Eisele
In collaboration with: G. Bilger, T. C. Röder, M. Sämann, J. R. Köhler, and J. H. Werner

The *ipe* has developed a laser doping process suitable for the production of full area emitters, as well as for selective emitters [1]. So far, the efficiency of solar cells with laser doped emitters was limited to η = 15.4 % [2]. Since then, we used phosphorus containing doping liquids as precursor layers prior to laser processing. These precursor layers have several drawbacks, such as high cost as well as the formation of inhomogeneous emitters due to local variations in thickness and composition.

In the present work, we replace the liquid precursors with sputtered phosphorus layers. A purpose developed 8” sputter target enables the deposition of homogeneous layers of atomic phosphorus on areas up to 6” in diameter. The deposition process permits the control of the layer thickness with a reproducibility of $\pm$ 1 nm. Replacing the liquid precursors by sputtered phosphorus layers results in a new record efficiency η = 18.9 % for crystalline silicon solar cells with full area laser doped emitters [3].

A conventional RF sputtering system modified with the purpose developed phosphorus target serves for depositing the layers. We use the target to intermediate target sputtering technique [4] for the preparation of the doping precursors. For laser doping experiments we vary the thicknesses of the dopant films as well as the laser parameters for laser doping. Experimental investigations demonstrate that the doping concentration in the laser treated emitter sensitively depends on the precursor layer thickness. Therefore, we precisely control the thickness in order to adjust the emitter doping concentration. We compare two different pulsed diode pumped solid state lasers #1 and #2, both emitting at a wavelength λ = 532 nm but with different pulse durations $\tau_{p\#1}$ = 10 ns and $\tau_{p\#2}$ = 65 ns.

Figure 1 depicts doping profiles, set #1 and set #2, of laser emitters fabricated with laser #1 and #2, measured by Secondary Ion Mass Spectrometry (SIMS). All emitters of set #1 exhibit a significantly higher maximum phosphorus surface concentration $C_{p,max}$, compared to set #2. The higher C_p,max of set #1 increases surface recombination and therefore reduces the influence of the recombination inside the emitter volume.

The longer pulse duration τ_{p2} = 65 ns of set #2 increases the melting time of the silicon surface, enabling the dopant atoms to diffuse longer into the melt. This results in a lower maximum phosphorus surface concentration $C_{p,max}$ and a deeper emitter depth z, compared to set #1. The lower $C_{p,max}$ enables a better surface passivation leading to smaller emitter saturation current densities J_{oe} and consequently higher solar cell efficiencies η.

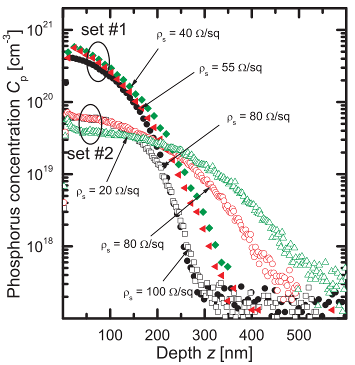

Figure 1:
Doping profiles of laser emitters, measured by SIMS. Filled symbols represent sample set #1, irradiated with laser pulse duration $\tau_{p1} \approx 10$ ns at different pulse energy densities E_p. Open symbols of set #2 stand for longer $\tau_{p2} \approx 65$ ns. The maximum phosphorus concentration $C_{p,max}$ of set #1 is about one magnitude higher than set #2, leading to higher surface recombination.

References:

[1] A. Esturo-Bretón, M. Ametowobla, J. R. Köhler, and J. H. Werner, in *Proc. 20th EU PVSEC* (WIP, Munich, Germany, 2005) p. 851

[2] T. C. Röder, P. Grabitz, S. J. Eisele, C. Carlsson, J. R. Köhler, and J. H. Werner, in *Proc. 34th IEEE Photov. Spec. Conf.* (IEEE, Piscataway, NJ, 2009) in press

[3] S. J. Eisele, T. C. Röder, J. R. Köhler, and J. H. Werner, Appl. Phys. Lett. **95**, 133501 (2009)

[4] G. Bilger and G. H. Bauer, Thin Solid Films **119**, 103 (1984)

Quantitative Electroluminescence Imaging

Author: A. Helbig
In collaboration with: T. Kirchartz and U. Rau**

When operated like an LED (light emitting diode), a solar cell will emit wavelength-dependent radiation, the so-called electroluminescence (EL). Detecting the EL with a camera [1] is well suited for large-area devices like solar cells since the image obtained provides spatially resolved information on solar cell properties. However, by integrating the EL spectrum in each camera pixel, the wavelength dependency is lost and with it significant information on cell parameters which determine the solar cell's performance under illumination.

According to the reciprocity theorem [2] the EL spectrum equals the product of the external quantum efficiency, the black body spectrum, and a wavelength independent factor determined by the junction voltage. Thus, the access to the EL spectrum detected in every camera pixel, requires two EL images measured with the same voltage applied but within different spectral ranges. The latter is easily accomplished by putting edge filters in front of the recording camera [3]. The pixel-wise ratio of the two EL images produces a contrast value in each pixel which, on the one hand, correlates with the slope of the detected EL spectrum and, on the other hand, eliminates voltage dependent parts of the EL intensity.

Figure 1 demonstrates that the transmission characteristics of the filters used determine the cell parameters which are retrievable from the contrast values [4]. We investigated a 4 cm^2 monocrystalline silicon solar cell with aluminum back contacts. The application of short-pass filters yields contrast values depending on the bulk diffusion length and the surface recombination velocity. Therefore, the cut-off wavelength of the filters has to be at least that small that radiation which was reflected by the back side of the cell is blocked. The interpretation of the contrast values only requires the

*Institute of Energy Research – Photovoltaics (IEF-5), Research Centre Jülich simulation of the quantum efficiency and spectral sensitivity of the detecting system. Figure 1a presents the surface recombination velocity map of the cell obtained by the application of the combination of a 1000 nm and a 950 nm short-pass filter. The diffusion length *L* is assumed to be *L* = 2000 µm. The surface recombination velocity at the point contacts is one order of magnitude higher than the one at the SiO_2 passivated surface next to the point contacts. Using long-pass filters transmitting radiation which was reflected on the back side leads to contrast values which reveal information on light trapping. Figure 1b displays the map of the back side reflection resulting from a contrast image representing the ratio of two EL images, one recorded without filter and one with an 1100 nm long-pass filter.

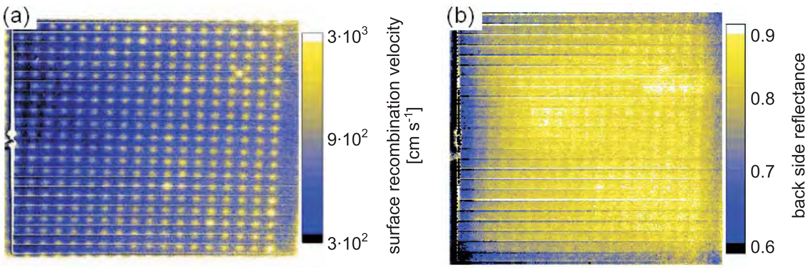

Figure 1:
a) Surface recombination velocity image calculated from the ratio of two EL images, one recorded with a 1000 nm and one with a 950 nm short-pass filter. The diffusion length is set to *L* = 2000 µm.
b) Back side reflectance image gained from the ratio of an EL image recorded without filter and one recorded with a 1100 nm long-pass filter.

References:

[1] T. Fuyuki, H. Kondo, T. Yamazaki, Yu Takahashi, and Y. Uraoka, Appl. Phys. Lett. **86**, 262108 (2005)
[2] U. Rau, Phys. Rev. B **76**, 085303 (2007)
[3] P. Würfel, T. Trupke, T. Puzzer, E. Schäffer, W. Warta, and S. W. Glunz, J. Appl. Phys. **101**, 123110 (2007)
[4] T. Kirchartz, A. Helbig, and U. Rau, Sol. Energy Mat. Sol. Cells **92**, 1621 (2008)

Laser Doped Selective Emitters yield 0.5% Efficiency Gain

Author: J. R. Köhler
*In collaboration with: S. J. Eisele, T. C. Röder, J. H. Werner, and P. Grabitz**

The patented *ipe* selective emitter (SE) laser doping process increases the efficiency η of monocrystalline industrial solar cells by $\Delta\eta$ = 0.5% absolute. The process uses only one additional laser processing step after furnace diffusion. A phosphosilicate glass layer on top of the emitter serves as doping precursor for the laser doping process. The average efficiency η of 125 x 125 mm^2 industrial solar cells with laser doped selective emitter is η = 18.0%, with a low standard deviation $\delta\eta$ = 0.05%. The best solar cell features an efficiency η = 18.1%. Table I presents the average values of efficiency η open circuit voltage V_{OC}, short circuit current density J_{SC} and fill factor *FF* of 10 selectively laser doped solar cells and 8 reference cells.

Table I: Laser doped SE yield a significant increase in efficiency by $\Delta\eta$ = 0.5% absolute as a result of less recombination in the emitter. Reduced *FF* of SE cells mainly results from non-optimized front grid design.

cell	η [%]	J_{sc} [mA/cm^2]	V_{oc} [mV]	*FF* [%]
selective	18.0	37.1	629	77.1
reference	17.5	36.1	619	78.4

A numerical simulation of the laser induced melting and recrystallization process compares lasers with different pulse durations. Figure 1a presents the increase of the depth of the molten silicon layer d_{melt} with laser pulse energy density E_P for different laser pulse durations τ = 10 ns to 200 ns. At the threshold energy E_{th} the surface of the silicon starts to melt. Larger pulse durations τ require more pulse energy density to melt the silicon surface, because more heat dissipates via heat diffusion into the silicon

*Solarwatt Cells GmbH, Heilbronn

wafer before the silicon starts to melt. After the pulse energy density E_P exceeded the threshold energy density E_{th} the melt depth d_m increases almost linearly with E_P. It reaches its maximum value if the temperature at the surface of the wafer exceeds the boiling or evaporation temperature of silicon $T_b \approx 2900$ K. Figure 1b shows that a melt depth $d_{melt} = 500$ nm requires a minimum pulse energy density of $E_P \approx 4$ J/cm^2 for a pulse duration $\tau \approx 20$ ns. Longer laser pulse durations require more pulse energy density for the same melt depth d_{melt}.

A processing time of $t_p = 1.3$ s for a 6 inch solar cell requires a laser with output power $P = 600$ W, if its pulse duration is $\tau = 50$ ns. A laser with $\tau = 200$ ns has to achieve an output power of $P = 1200$ W for the same throughput. The output power of conventional rod laser systems is limited to about $P = 100$ W. Despite their longer pulse duration only disc lasers have the potential to achieve the necessary output power with average powers in the multi 100 W-range.

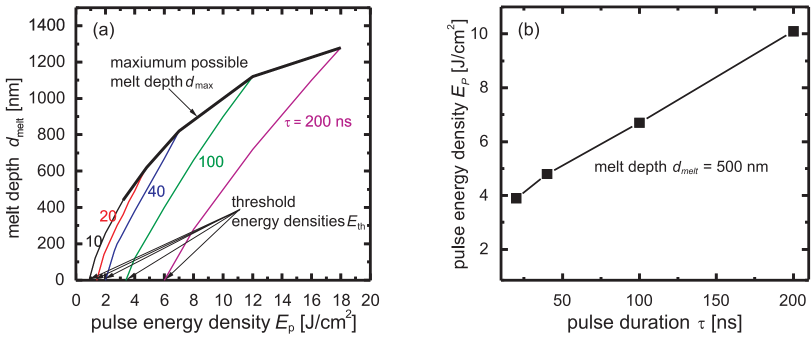

Figure 1:
a) Numerical simulation of laser doping process indicates a strong increase of the maximum possible melt depth d_{max} for increasing laser pulse durations τ.
b) For a constant melt depth $d_{melt} = 500$ nm, the required pulse pulse energy density E_p increases with pulse duration τ.

References:

[1] S. Eisele, T. Röder, J. R. Köhler, and J. H. Werner, Appl. Phys. Lett. **95**, 133501 (2009)

Advanced Front Grid Optimization Method for Solar Cells

Author: G. Kulushich
In collaboration with: R. Zapf-Gottwick and J. H. Werner

The efficiency of solar cells is affected by different power losses. Important power losses for industrial screen printed solar cells are optical and electrical losses associated with the front grid design. The conventional optimization method [1, 2] does not regard the fact that not only the losses, but also the voltage and the current change when changing the front grid design. This assumption contradicts the purpose of the optimization.

The present contribution shows a simple way of calculating the maximum power point voltage V_{mpp}, the maximum power point current I_{mpp}, and the conversion efficiency η for different front grid design. This method allows to calculate the "ideal" maximum power point current density J_{mpp}*, the "ideal" maximum power point voltage V_{mpp}*, and the "ideal" efficiency η* for a "stripped off" solar cell without front grid power losses. Figure 1 shows the scheme of the advanced front grid optimization. (a The method starts with a real solar cell with not-optimized front grid design. The front grid parameters and the electrical characteristics of the starting cell are known. b) The

(a) Real solar cell (b) Stripping off front grid (c) Dressing on front grid

Figure 1:
Scheme of advanced front grid optimization approach. a) Starting point is real solar cell. b) Stripping off front grid. c) Calculating efficiency for redressed solar cell with any design.

second step is theoretically "stripping off" the solar cell front grid and calculating J_{mpp}*, V_{mpp}*, and η*. c) The third step is theoretically "dressing on" the cell with any front grid design and calculating J_{mpp}, V_{mpp}, and η by varying the front grid design parameters. By plotting efficiency contour plots, the advanced front grid optimization method is able to determine the optimal front grid design for the starting solar cell. The advantage of the present optimization method is that it takes into account the influence of the front grid design on J_{mpp} and V_{mpp}.

Figure 2 depicts efficiency η contour plots for different finger widths and finger numbers. About Δη > 0.2 % absolute efficiency gain is calculated for an optimal front grid design with more than 85 fingers of width w_f < 70 µm, yielding an efficiency η = 17.5 %. In this calculation, the finger height h_f = 20 µm is constant which is feasible with fine-line printing of finger widths w_f < 70 µm.

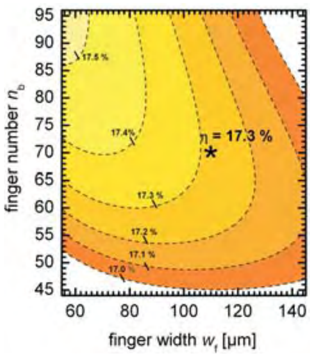

Figure 2:
Simulation of efficiency η for optimizing finger width w_f and number of fingers n_f. Front grid consists of two busbars of width w_b = 1.5 mm and height h_b = 20 µm. Front grid with more than 85 fingers with w_7 < 70 µm promise efficiency η > 17.5 %. Fine-line printing promises Δη > 0.2 % absolute efficiency gain. Star at position n_f = 70 and w_f = 110 µm represents conventionally feasible screen printed fingers.

References:

[1] M. A. Green, *Solar Cells: Operating Principles, Technology, and System Applications* (Prentice-Hall, Upper Saddle River, NJ,1981) p.153

[2] A. R. Burgers, *New Metallisation Patterns and Analysis of Light Trapping for Silicon Solar Cells*, PhD Thesis (Energieonderzoek Centrum Nederland, Petten, 2005) p.32

In-situ Series Connection for Thin Film Photovoltaic Modules

Author: R. Merz
In collaboration with: M. B. Schubert

Amorphous silicon (aSi) based thin film solar cells enable roll-to-roll manufacturing of photovoltaic modules on inexpensive substrate foil. Monolithic series connection of single cell stripes increases the output voltage of the module and reduces resistive losses by keeping its output current low. For an optimum series connection, the interconnection gap, i.e. the dead area where the front contact of each cell stripe connects to the back contact of the adjacent one, must be as small as possible. In addition, only resistive losses $P_{TCO} \sim J_{ph}(w_{act})^3$ in the transparent front contact (TCO), rising with the third power of the active cell width w_{act}, significantly contribute to the total interconnection losses F. Figure 1a presents a schematic cross section of the *in-situ* series connection (ISSC) of three n-i-p solar cell stripes in substrate configuration. Masking wires separate neighbouring cell stripes during the deposition of the Ag/ZnO back contact stack.

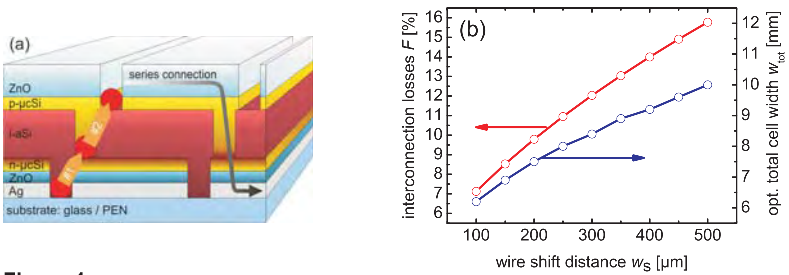

Figure 1:
a) Cross section of the *in-situ* series connection. The arrows describe the shift sequence of the shading wires. First wire shift #1 after Ag, ZnO and n-µcSi deposition masks the back contact layer stack. The second shift #2 after i-aSi deposition opens access to the back contacts of cells for series connection during p-µcSi and ZnO front contact deposition. b) Calculation of the total ISSC losses F in dependence of the wire shift distance w_s, with resulting optimum cell width w_{tot}. At w_s = 250 µm, total interconnection losses drop to $F < 10$ %.

A first wire shift #1 after growing the microcrystalline n-type silicon (n-µSi), masks the back contacts of the cells during plasma enhanced chemical vapour deposition (PECVD) of the undoped (intrinsic) aSi absorber layer. The low conductivity of this undoped material also isolates the cell stripes from each other. A second wire shift before p-type p-µcSi and top ZnO:Al deposition opens access to the back contacts of the cells for the final series connection and at the same time isolates the front contacts of adjacent cells. Figure 1b calculates the minimum interconnection losses F of the ISSC technology as a function of the wire shift distance ws and displays the corresponding total cell width w_{tot}. For wire shifts w_s < 250 µm and an optimum cell width w_{tot} = 8 mm, the total ISSC losses drop to F < 10 %.

Figure 2 compares the measured current-voltage (I-V) characteristics of a 10-cell ISSC module with the characteristics calculated from single cell data. Dead area and resistive ZnO losses sum up to total interconnection losses F = 15 %. The module output voltage V_M = 9 V and its fill factor FF_M = 49 %, close to FF_C = 50 % of the reference cells, indicate successful ISSC with no major shunts.

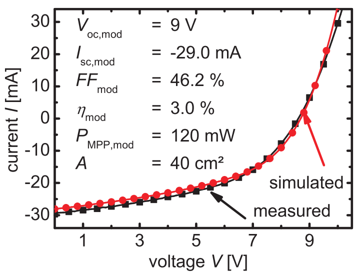

Figure 2:
The measured I-V characteristics of an ISSC module (sqares) agree well with the corresponding I-V curve (dots), recalculated from reference cell data by taking into account the power loss due to the dead area and the resistive loss in the top ZnO layer. The reference cells were deposited under similar conditions as the module, but without shifting the shading wires.

References:

[1] R. Merz, M. M. Adachi, M. B. Schubert, J. H. Werner, in *Proc. 23rd Europ. Photovolt. Solar Energy Conf.*, edited by D. Lincot, H. Ossenbrink, P. Helm (WIP, München, 2008) p. 2411.

[2] Y. Gupta, H. Liers, S. Woods, S. Young, R. Deblasio, L. Mrig, in *Conf. Rec. 16th Photovolt. Spec. Conf.* (IEEE, San Diego, USA, 1982) p. 1092.

Analysis of Heavily Doped Emitters of Silicon Solar Cells

Author: V. Nguyen
In collaboration with: M. Reuter, P. Gedeon, and R. Zapf-Gottwick

The heavily n-type doped emitter of commercial screen-printed (SP) multicrystalline silicon (mc-Si) solar cells has an emitter sheet resistance between $55 \leq \rho_e \leq 65\ \Omega$/sq, at a phosphorus surface concentration of $N_P \approx 10^{21}$ cm^{-3}, and a depth $d \approx 350$ nm. The high surface concentration provides a low contact resistance for SP metallization and getters metallic impurities during diffusion for bulk lifetime improvement of low quality block cast mc-Si materials. This work shows the heavily doped emitter to be the main reason for low open circuit voltages V_{OC} of SP mc-Si solar cells. We use the Alamo-Swanson analytical model [1] for current transport in heavily doped emitters to analyze the emitter saturation current density J_{0e} for emitter sheet resistances $\rho_e = 60$, 80 and 100 Ω/sq. The interface recombination velocity between plateau and tail region derives from the the high-low junction model [2]. We further apply the Alamo-Swanson model to evaluate the contribution of emitter surface, emitter plateau and emitter tail to J_{0e}. We found that surface and emitter plateau recombination mainly contribute to J_{0e}.

Figure 1 shows the phosphorus depth profiles for the 60 Ω/sq, 80 Ω/sq and 100 Ω/sq emitters on c-Si wafers, measured by secondary ion mass spectrometry (SIMS). The phosphorus surface concentration N_P of all three emitters exceeds 10^{21} cm^{-3}. However, the active concentration of P in Si saturates at $C_P = 2.5 \times 10^{20}$ cm^{-3} as measured by Electrochemial Capacitance Voltage (ECV) analysis.

Figure 2 shows the calculated J_{0e} and V_{OC} of three emitter profiles for a varying surface recombination velocity S. The 60, 80 and 100 Ω/sq emitters set an upper limit for open-circuit voltages of c-Si solar cells at V_{OC} = 640, 650 and 660 mV. The emitter saturation current density J_{0e} remains nearly constant for $S < 10^4$ cm/s, thus better surface passivation will not improve V_{OC}.

Figure 3 shows the contribution of emitter surface, plateau, and tail to the overall J_{0e}. For all analyzed emitters the surface recombination exceeds the bulk recombination. The emitter plateau contributes to more than 95 % (absolute) of recombination of the emitter bulk.

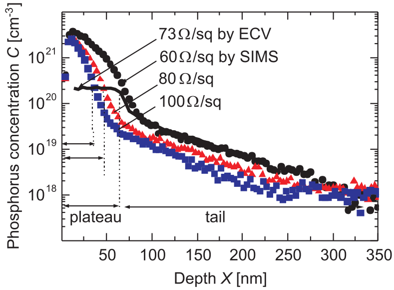

Figure 1:
Phosphorus depth profiles by SIMS for 60 Ω/sq, 80 Ω/sq and 100 Ω/sq emitters on c-Si wafers and by ECV for 73 Ω/sq emitter.

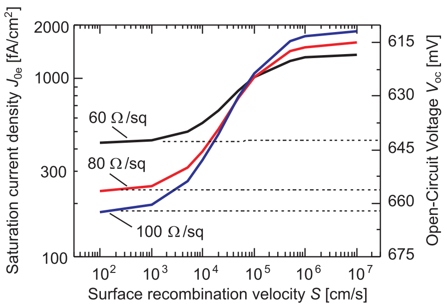

Figure 2:
Calculated emitter saturation current density J_{0e} and open circuit voltage V_{OC} of 60, 80 and 100 Ω/sq emitters for different surface recombination velocities S.

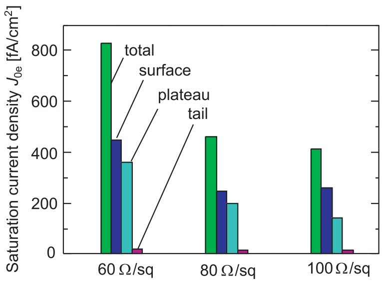

Figure 3:
Contribution of plateau, tail, and surface recombination to emitter saturation current density for a surface recombination velocity $S = 2 \times 10^4$ cm/s. Recombination occurs mostly at the emitter surface and in the heavily doped plateau region.

References:

[1] J. A. del Alamo and R. M. Swanson, IEEE Trans. Electrons Devices **ED-31**, 1878 (1984).

[2] A. Rohatgi and P. Rai-Choudhury, IEEE Trans. Electrons Devices **ED-31**, 596 (1984).

Photovoltaic Fluorescent Collector with Solar Cells at the Back Side

Author: L. Prönneke
*In collaboration with: G. C. Gläser and U. Rau**

Fluorescent collectors (FCs) consist of a dielectric material including dye molecules, which absorb incoming photons and emit them spatially randomized at lower energy. Total internal reflection guides part of the emitted rays to the collector edges. A photonic structure (PS) on top of the FC increases the amount of side-guided photons, because of its energy selective performance. Regarding this side-guiding behavior, the main interest of research lies in applying solar cells to the FC sides [1,2]. Unfortunately, this application needs a complicated set-up considering industrial requirements.

In contrast, the present contribution introduces a novel set-up of a FC with solar cells partially covering the back side. In numerical simulations of ideal FCs in photovoltaic systems we already proposed the possibility of partially covering the back side with solar cells while achieving the same photon collection as in the side-mounted systems [3]. Now, we present an experimental set-up with an FC on top of the solar cell increasing the photon collection.

Figure 1a compares line-scans of three performed Laser Beam Induced Current (LBIC) measurements with a wavelength of 406 nm: An amorphous silicon solar cell alone, with an FC on top, and with an FC and an additional PS filter on top. Obviously, for the solar cell alone, the photovoltaic active area is restricted to the cell. Altogether, the system collects the current I_{coll} = 8.5 mA. The FC applied on top of the solar cell decreases the current induced above the cell significantly. However, the larger photovoltaic active area compensates this loss and the overall collected current increases to I_{coll} = 9.1 mA. Compared to the FC alone, the application of the PS filter not only increases the current collected above the cell but also the

*Institute of Energy Research – Photovoltaics (IEF-5), Research Centre Jülich

photovoltaic active area. Thus, the FC combined with a PS gains 95 % more current (I_{coll} = 16.6 mA) than the solar cell alone. In Fig. 1b we present simulations of the line-scans. A Monte-Carlo ray-tracing simulation calculates the current for realistic components. The simulation fits the measurement, but shows slightly better values, which result from the assumption of a perfect Lambertian reflector and an ideal optical coupling above the solar cell.

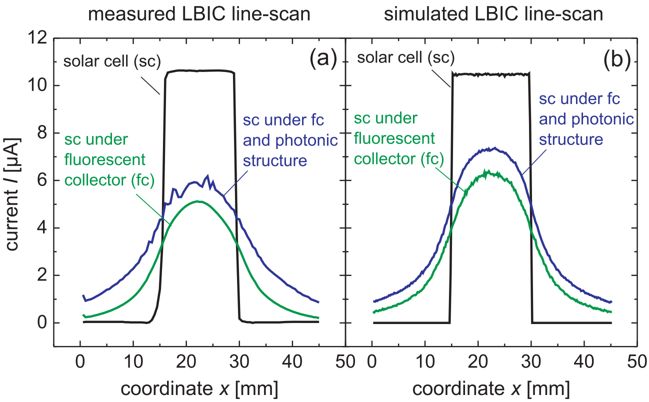

Figure 1:
a) Comparison of LBIC lines-cans. Above the solar cell, the application of the FC as well as the PS decreases the current significantly. However, both components compensate this loss by enlarging the photovoltaic active area. The overall collected current I_{coll} increases from 8.5 mA (solar cell alone) to 9.1 mA (FC applied) and 16.6 mA (FC and PS on top). b) Monte-Carlo ray-tracing simulation results for realistic components. The Lambertian reflector and the optical coupling are assumed to be ideal, which results in better values for the current than in the measurement.

References:

[1] L. H. Slooff, A. R. Burgers, T. Budel, et al., Phys. Stat. Sol. Rapid Research Lett. **2**, 257 (2008).
[2] J. C. Goldschmidt, M. Peters, L. Prönneke, et al., Phys. Stat. Sol. (a) **1 – 11**, 2811 (2008).
[3] L. Prönneke, U. Rau, Proc. Soc. Photo-Optical Instrument. Eng. **7002**, 70020U (2008).

18.9% Efficient Full Area Laser Doped Silicon Solar Cell

Author: T. C. Röder
In collaboration with: S. J. Eisele, J. R. Köhler, and J. H. Werner

This contribution reports on a full area laser doped emitter (LDE) solar cell with record energy conversion efficiency $\eta = 18.9\%$*, achieved by combining laser doping with conventional silicon solar cell processing [1]. At present, the efficiency η is limited by the short circuit current density J_{sc} = 35.2 mA/cm^2 due to the non-textured cell surface and not by the LDE, as proven by the high open circuit voltage V_{oc} = 677 mV.

Figure 1 presents the layout of the record LDE solar cell. First, a sputtering process deposits a 60 nm pure phosphorus precursor layer on top of the wafer. Then, laser irradiation of a pulsed Nd:YAG laser melts the silicon surface up to a depth of about one micron. While the silicon is liquid, phosphorus atoms from the precursor layer diffuse into the melt, creating the n-type emitter and thus the pn-junction at the surface of the p-type silicon wafer. The front and rear sides of the wafer use SiO_2 passivation for low surface recombination. The front contacts consist of a photolithographically opened grid through the oxide and a subsequent evaporation of Ti/Pd/Ag. A stack of 35 nm ZnS and 100 nm MgF_2 at the front side provides a double layer anti-reflection coating (ARC).

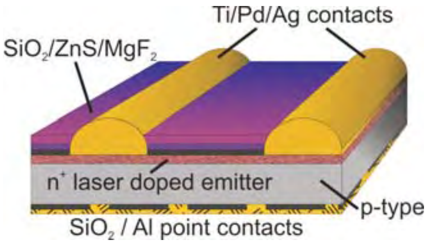

Figure 1:
Scheme of η = 18.9% efficient laser doped emitter solar cell. A double layer of 35 nm ZnS and 100 nm MgF_2 serves as anti-reflection coating. Silicon dioxide passivates the front and rear providing a low surface recombination. Contact holes through the SiO_2 form the Al rear contact.

The aluminum rear metallization contacts the substrate via a network of photolithographically opened contact holes through the rear SiO_2 passivation layer.

Figure 2 presents the emitter saturation current densities J_{oe} of LDE samples irradiated with different laser pulse energies. The J_{oe} - values are extracted from lifetime measurements, using the approach proposed by Cuevas [2]. The emitter saturation current densities J_{oe} increase monotonically with decreasing emitter sheet resistance ρ_s. This behavior is related to the increase in doping and thus Auger recombination inside the emitters. The lowest saturation current density J_{oe} = 88 fA/cm^2 corresponds to a sheet resistance ρ_s = 124 Ω/□. This value is comparable to high efficiency silicon solar cells. Thus, we conclude that laser doping does not lead to one dimensional, two dimensional or three dimensional lattice defects such as SiP-clusters, dislocations, or grain boundaries.

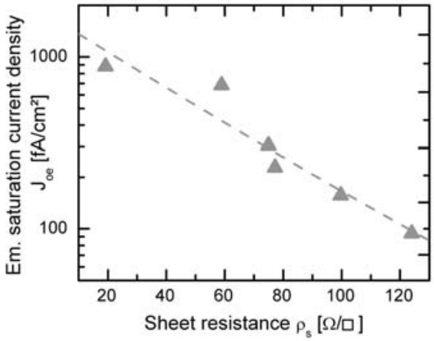

Figure 2:
Emitter saturation current density J_{oe} extracted from lifetime measurements. Increasing sheet resistance ρ_s decreases J_{oe} due to the lower Auger recombination inside the emitters. The highest ρ_s = 124 Ω/□ yields J_{oe} = 88 fA, showing the high quality of LDE.

*independently confirmed by ISE CalLab under standard test conditions

References:

[1] S. Eisele, T. Röder, J. R. Köhler, and J. H. Werner, Appl. Phys. Lett. **95**, 133501 (2009)

[2] A. Cuevas, Sol. Energy Mater. Sol. Cells, **57**, 277 (1999)

Sputtered and Laser Recrystallized Phosphorus Doped ZnO

Author: M. Saemann
In collaboration with: S. J. Eisele and G. Bilger

Phosphorus activation in phosphorus doped zinc oxide (ZnO:P) requires rapid thermal annealing at temperatures above 800°C [1] and is at odds with substrate degradation and out-diffusion of atoms. This contribution investigates the phosphorus incorporation in ZnO after laser irradiation by X-ray diffraction (XRD) and secondary ion mass spectroscopy (SIMS). Short laser pulses heat the ZnO film to momentary high temperature without damaging the substrate. XRD measures a relaxation of film strain after laser irradiation. SIMS confirms a liquid ZnO phase during laser irradiation from the diffusion profile of the phosphorus atoms. A line-focused frequency-tripled pulsed neodymium doped yttrium aluminum garnet (NdYAG) laser with wavelength λ = 355 nm and pulse duration τ_p = 65 ns irradiates the sample with pulse frequency f = 20 kHz and pulse energy densities between E_p = 0.73 J/cm^2 and 0.83 J/cm^2.

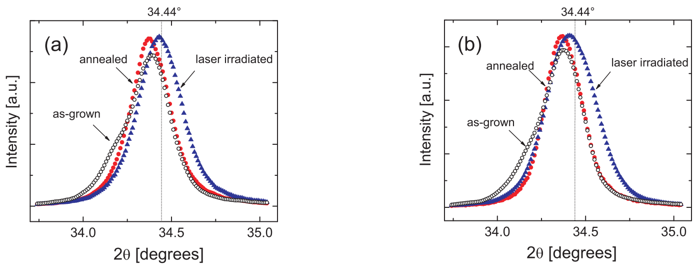

Figure 1:
XRD signature of the (0002) peak of as-grown (open circles), annealed (full circles) and laser irradiated (triangles) ZnO:P layers. a) Laser irradiation with pulse energy density E_p = 0.78 J/cm^2 shifts the 2θ peak position from 2θ = 37.37° to 34.43°. b) Higher E_p = 0.83 J/cm^2 causes microcracks and broadens the FWHM.

Figures 1a and 1b present the (0002) XRD pattern of glass/ZnO/ZnO:P layer stacks as-grown, annealed at 500°C, and after laser irradiation. Further crystalline phases are not found.

The shift of the peak position proves that laser irradiation locally melts the ZnO layers and relieves intrinsic biaxial stresses to the relaxed bulk value ($2\theta = 34.44°$) during recrystallization. A pulse energy density $E_p = 0.73$ J/cm^2 causes no measurable shift of the 2θ peak. The threshold pulse energy density for melting the layers is $E_p = 0.78$ J/cm^2. Pulse energy densities above $E_p = 0.83$ J/cm^2 induce microcracks, indicated by an increase of the full-width-at-half-maximum (FWHM) of the (0002) XRD peak. Figure 2 shows SIMS profiles of laser irradiated ZnO:P films with pulse energy densities $E_p = 0.73$ J/cm^2 to 0.83 J/cm^2. The phosphorus concentration in the films amounts to $n_P = 5 \times 10^{20}$ cm^{-3}. Target-to-Intermediate-Target [2] sputtering enables homogeneous P doping over the entire film thickness. The valley in the ZnO profile of the sample irradiated with $E_P = 0.73$ J/cm^2 at a depth $z = 240$ nm indicates an interface resulting from only partial melting of the ZnO:P layer. This finding is consistent with XRD results, which could not observe a relaxation of the stressed layer. The slopes of the phosphorus profiles towards the underlying intrinsic ZnO buffer layer at depths $z = 400$ to 700 nm decrease with increasing pulse energy density. Therefore, a liquid phase must be present at this interface, which enhances the diffusion of phosphorus.

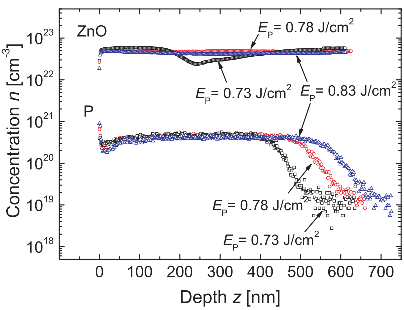

Figure 2:
SIMS depth profiles of laser irradiated ZnO:P films. The ZnO profile of the $E_P = 0.73$ J/cm^2 irradiated sample shows an interface at $z = 240$ nm, indicating only partial melting of the ZnO:P layer. The slopes of the P profiles towards the intrinsic ZnO buffer layer decrease with increasing E_P. A liquid phase must be present at this interface, which enhances the diffusion of P atoms.

References:

[1] K.-K. Kim, H.-S. Kim, D.-K. Hwang, J.-H. Lim, and S.-J. Park, Appl. Phys. Lett. **83**, 63 (2003).

[2] G. Bilger, G. H. Bauer, Thin Solid Films **119**, 103 (1984).

Amorphous Silicon p-i-i-n Photodetectors for Point-of-Care Testing

Author: M. Saemann and M. B. Schubert
In collaboration with: D. Furin[1], J. Thielmann[2], A. Pfäfflin[3], G. Proll[1], C. Harendt[2], G. Gauglitz[1], and E. Schleicher[3]

Modern medical diagnostics requires Point-Of-Care Testing (POCT) systems in clinical or outpatient environments. Main advantages are quick test results within a few minutes and the possibility to discharge a patient from hospital after surgery while critical parameters, like inflammation or cardiovascular markers, can still be monitored at home.

Here we introduce amorphous silicon (aSi) based photodetectors into a POCT system and present the successful monitoring of C-reactive protein (CRP) and D-dimer in physiologically relevant concentrations. The direct optical and label-free detection is based upon the Reflectometric Interference Spectroscopy (RIfS) [1] which observes interferences in an optical multilayer system. If proteins in the patient's blood interact with antibodies, fixed on top of the multilayer system, they change the optical thickness of the top layer. This change induces a wavelength shift of the interference spectrum. Spectrally selective photodetectors with p-i-i-n structure have the ability to detect this shift, and thus replace the so far needed spectrometer. Current-voltage characteristics and the spectral selectivity of such photodetectors were published in ref. [2]. Current-to-frequency conversion of the photodetector response by an Application Specific Integrated Circuit (ASIC) ensures accurate recording over a wide sensitivity range. Figure 1 presents three subsequently performed measurements of CRP with a concentration of 5 mg/l. C-reactive protein is an acute-phase protein, which rises quickly in response to inflammations. At an externally supplied read-out voltage V = -7.7 V on the photodiodes, the ASIC chip measures the photocurrent and converts it to a frequency. The exponential increase at t = 250 s represents bonding of CRP to CRP-antibodies on the surface and the resulting change in optical thickness.

[1]Institut für Physikalische und Theoretische Chemie, Universität Tübingen
[2]Institut für Mikroelektronik, Stuttgart
[3]Universitätsklinikum und Medizinische Fakultät, Universitätsklinikum Tübingen

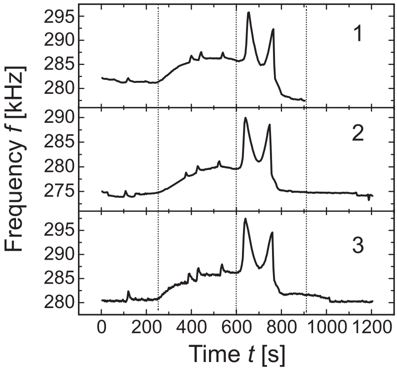

Figure 1:
Three subsequently performed measurements of 5 mg/l C-reactive protein (CRP) in buffer solution. While recording a baseline, Ovalbumin tests the surface against unspecific bindings. During the association phase, CRP covalently bonds to CRP-antibodies on the surface. During the regeneration phase indicated by two intensive peaks, CRP is dissolved and washed from the surface. The signal returns to the baseline at the end of each measurement and the surface is ready for the next measurement.

Figure 2 shows a successful D-dimer detection with a concentration of 5.5 mg/l. D-dimer is a fibrin degradation product and indicates activated blood coagulation. Monitoring D-dimer in a patient's blood helps to diagnose pulmonary embolism or thrombosis.

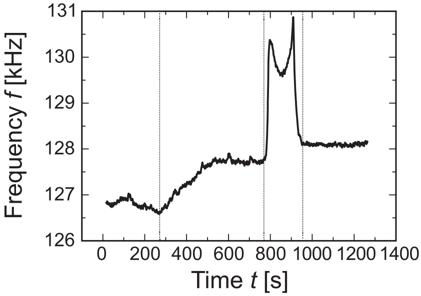

Figure 2:
Detection of 5.5 mg/l D-dimer at an applied read-out voltage V = -7.7 V and illumination at wavelength λ = 530 nm. Measurement starts with recording a baseline. During the association phase D-dimer interacts with D-dimer antibodies on the substrate surface. Two intense peaks mark the regeneration phase which dissolves the bonds. The functionalized surface is not recoverable after D-dimer detection, yet.

References:

[1] G. Gauglitz, A. Brecht, G. Kraus, and W. Nahm, Sensor. Actuat. B-Chem. **11**, 21 (1993).

[2] M. Sämann, L. Steinle, and M. B. Schubert, J. Non-Cryst. Solids **354**, 2575 (2008).

Improved Concept for Industrial Screen Printing Line

Author: R. Zapf-Gottwick
In collaboration with: J. Cichoszewski, M. Mühlbauer, V. Nguyen, J. H. Werner, T. Schlenker, and D. Manz**

The present contribution reports on a novel concept for an industrial screen printing line for metallization of solar cells established at *ipe*. The line implements three improved components: i) a high quality screen printer which prints two solar cells at the same time, thus increasing printing speed by 100 %, ii) a drying furnace with a paternoster principle, thus using much smaller foot print than conventional furnaces, iii) a firing furnace with a new transport principle, using quartz glass rolls instead of a metal conveyor belt, thus decreasing energy consumption and metal contamination. We designed and investigated this prototype of industrial screen printing line. Processing the same type of cells in our line gives similar, improved results when compared to a conventional industrial line.

The main optimization work is done on the firing furnace. The characteristics of a typical firing profile follows the conditions given by the contents of the screen printing paste: i) removal of the organic binders at about 400 °C, ii) melting of the glass frit and the mechanical bonding to Si, iii) sintering of the metal particles. Figure 1 shows different temperature profiles in the firing furnace. Higher roll velocities imply that the maximum peak temperature

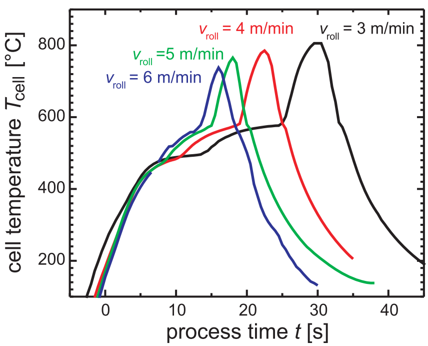

Figure 1: Measured temperature profiles in firing furnace: maximum temperature on cell $T_{p\text{-}cell}$ decreases with higher roll velocity v_{roll}. Set-point temperature in peak zone T_{peak} = 820 °C is kept constant; variation is in roll velocity v_{roll}.

*Manz Automation AG, Reutlingen

T_{cell} on the cell is getting lower and the peak width is getting smaller. Optimization is done in different firing temperatures and velocities maximizing the measured electrical values. The new screen printing line at *ipe* is a powerful base not only for industrial fabrication but also for developing alternative process steps in research and proving them with industrial metallization. Printer, dryer and firing furnace allow for a good handling, controlling and homogeneity of the metallization process. Latest processed and produced solar cells from *ipe* show in house measured efficiencies of η = 17.2 % on mono crystalline solar cells and η = 16.4 % on multi crystalline cells each with an industrial size of 156 x 156 mm^2.

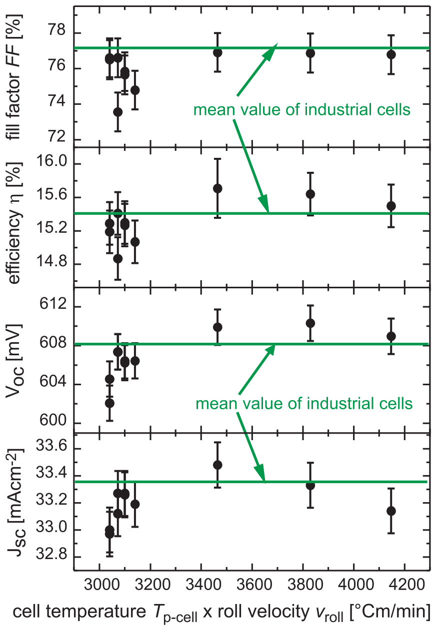

Figure 2:
Solar cells results of cells processed by novel screen printing line in comparison to cells metallized in a conventional industrial line. The product of $T_{p\text{-}cell}$ and v_{roll} gives an optimization window for efficiency and fill factor *FF*, short circuit current J_{sc} and open circuit voltage V_{oc}: a narrow one for J_{sc} in the range of 3200 °Cm/min < T_{cell} v_{roll} < 3700 °Cm/min and an extended one for V_{oc} in the range of 3300 °Cm/min < T_{cell} v_{roll} < 4200 °Cm/min.

Annual Energy Yield of Photovoltaic Systems

Author: B. Zinßer
In collaboration with: G. Makrides, G. E. Georghiou, M. B. Schubert, and J. H. Werner*

At present, several different photovoltaic (PV) technologies share the market, or attempt to enter it. End users and investors want to know how much energy each of those PV technologies produces, and which technology fits best for a specific application and location. For monitoring their energy yield, the *ipe* operates the PV systems shown in Fig. 1a in Nicosia (Cyprus), and the ones presented in Fig. 1b in Stuttgart (Germany). The twelve fixed mounted systems at each location use mono- and multi-crystalline silicon and the thin film technologies amorphous Si, CdTe and $Cu(InGa)Se_2$ [1].

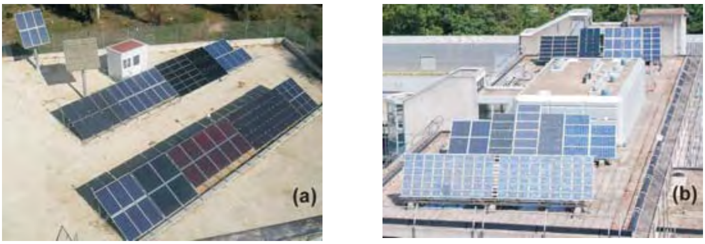

Figure 1: a) PV systems in Nicosia (Cyprus), b) PV systems in Stuttgart (Germany).

Figure 2a shows the annual energy yield E_{AC} normalized to the rated power $P_{N,rated}$ of the PV generators. This normalization is important for the return on investment because nowadays customers pay for the rated power. For a more detailed scientific comparison of the PV technologies [2], Fig. 2b uses the actually measured power from outdoor field operation $P_{N,field}$ to normalize E_{AC}. Remarkable differences occur for the amorphous silicon

*University of Cyprus - Photovoltaic Technology systems whose $P_{N,field} < P_{N,rated}$. Taking into account the error bars which mainly arise from uncertainties in rated power and solar irradiance, a winning PV technology is not discernible yet.

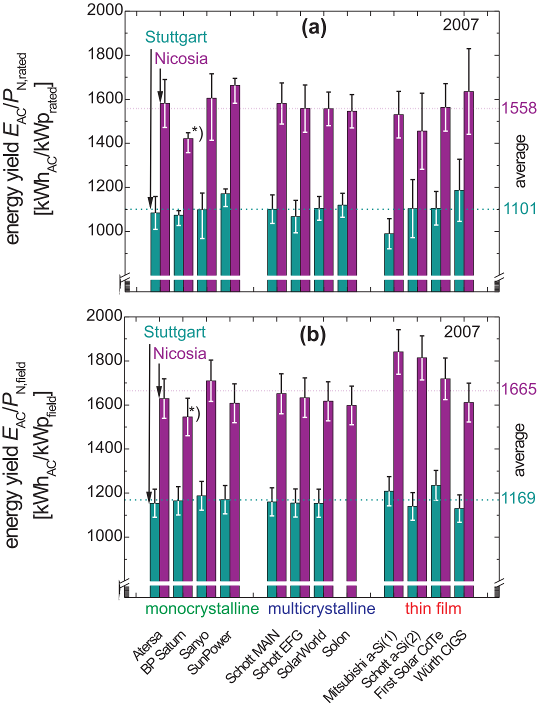

Figure 2:
Annual energy yield E_{AC} of different PV systems, a) normalized to their rated power, b) normalized to the power deduced from outdoor field operation. The error bars are mainly due to module power tolerance, and much bigger than the differences in E_{AC}. All crystalline Si technologies show very similar E_{AC}, while the amorphous Si systems exhibit a higher apparent yield in b) due to $P_{N,field} < P_{N,rated}$. *) This system suffers from some shadow in the morning.

References:

[1] Live data web page: www.ipe.uni-stuttgart.de/pvsystem.

[2] B. Zinßer, G. Makrides, M. Schubert, G. E. Georghiou, and J. H. Werner, in *Proc. 24th Europ. Photovolt. Sol. En. Conf.* (WIP-Renewable Energies, München, Germany, 2009) in print.

Publikationen
Publications

Results from Multipoint Alignment Monitoring Using the New Generation of Amorphous Silicon Position Detectors
J. Alberdi, P. Arce, J.M. Barcala, E. Calvo, A. Ferrando, M.I. Josa, A. Molinero, J. Navarrete, J.C. Oller, C. Yuste, A. Calderon, G. Gomez, F.J. Gonzales-Sanchez, C. Martinez-Rivero, F. Matorras, T. Rodrigo, P. Ruiz-Arbol, M. Sobron, I. Vila, A.L. Virto, C. Köhler, B. Lutz, M. B. Schubert, and J. H. Werner,
Nuclear Instruments and Methods in Physics **A593**, 608 (2008)

Texturization By Metal-Assisted Chemical Etching For Silicon Solar Cells
J. Cichoszewski, and M. Lipinski,
in *The First International Forum on Multidisciplinary Education and Research for Energy Science* (Tokyo Institute of Technology, Tokyo, 2008) p. 35

Bifacial Solar Cells with Selective B-BSF by Laser Doping
C. Duran, S. J. Eisele, T. Buck, R. Kopecek, J. R. Köhler, and J. H. Werner,
in *Proc. 24th Europ. Photovolt. Solar Energy Conf.* (WIP, Munich, 2009) in press

0.8 % Higher Efficiency by Low Temperature Back Contact
C. Ehling, R. Merz, J. W. Müller, M. Hlusiak, P. J. Rostan, J. H. Werner, and M. B. Schubert,
in *Proc. 23rd Europ. Photovolt. Solar Energy Conf.*, eds. D. Lincot, H. Ossenbrink, P. Helm (WIP, Munich, 2008) p. 1657

0.8 % Efficiency Gain by Low Temperature Back Contact
C. Ehling, R. Merz, J. W. Müller, M. Hlusiak, J. H. Werner, and M. B. Schubert,

in *The First International Forum on Multidisciplinary Education and Research for Energy Science* (Tokyo Institute of Technology, Tokyo, 2008) p. 11

0.4% Absolute Efficiency Gain by Novel Back Contact
C. Ehling, M. B. Schubert, R. Merz, J. Müller, M. Hlusiak, P. J. Rostan, and J. H. Werner,
Sol. Energy Mater. Sol. Cells **93**, 707 (2009),
doi:10.1016/j.solmat.2008.09.036

a-SiC:H Passivation for Crystalline Silicon Solar Cells
C. Ehling, J. H. Werner, and M. B. Schubert,
phys. stat. sol. (c) **x**, xx, (2009) in press

Thermally Stable a-$Si_{1-x}C_x$:H Passivation Layers
C. Ehling, G. Bilger, and M. B. Schubert,
in *Proc. 24th Europ. Photovolt. Solar Energy Conf.* (WIP, Munich, 2009) in press

Development of an Integrated Direct Optical Biosensor for Point of Care Testing
D. Furin, F. Pröll, M. Sämann, J. Thielmann, K. Körner, A. Pfäfflin, G.Proll, H. Richter, L. Steinle, C. Harendt, W. Osten, E. Schleicher, M. Schubert, and G. Gauglitz,
in *Proc. 20th International Congress of Clinical Chemistry and Laboratory Medicine* (IFCC, Fortaleza, 2008)

18.9% efficient full area laser doped silicon solar cell
S. J. Eisele, T. C. Röder, J. R. Köhler, and J. H. Werner,
Appl. Phys. Lett. **95**, 133501 (2009)

18.9% Efficient Silicon Solar Cell with Laser Doped Emitter
S. J. Eisele, T. C. Röder, M. Ametowobla, G. Bilger, J. R. Köhler, and J. H. Werner,
in *Proc. 34th Photovoltaic Specialists Conf.* (IEEE Publishing Service, Piscataway, NY, 2009) in press

Characterization of Nanometer Thin Sputtered Phosphorus Layers for Laser Doping of Solar Cells
S. J. Eisele, M. Sämann, and G. Bilger,
in *Proc. ALC´09* (Maui, Hawaii, 2009) in press

Phosphorus Sputtered Laser Doped Emitters
S. Eisele, M. Ametowobla, G. Bilger, J. R. Köhler, and J. H. Werner,
in *Proc. 23rd Europ. Photovolt. Solar Energy Conf.*, eds. D. Lincot, H. Ossenbrink, P. Helm (WIP, Munich, 2008) p. 1737

Phosphorus Sputtered Laser Doped Emitters
S. Eisele, M. Ametowobla, G. Bilger, J. R. Köhler, and J. H. Werner,
in *The First International Forum on Multidisciplinary Education and Research for Energy Science* (Tokyo Institute of Technology, Tokyo, 2008) p. 13

Rugate Filter for Light-Trapping in Solar Cells
S. Fahr, C. T. Ulbrich, T. Kirchartz, U. Rau, C. Rockstuhl, and F. Lederer,
Opt. Express **16**, 9332 (2008)

Optimization of Rugate Filters for Ultra Light-Trapping in Solar Cells
S. Fahr, C. T. Ulbrich, T. Kirchartz, U. Rau, C. Rockstuhl, and F. Lederer,
in *Photonics for Solar Energy Systems II*, eds. by A. Gombert, (Proc. SPIE **7002**, Strasbourg, 2008) 70020B, doi:10.1117/12.781235

Theoretical and Experimental Analysis of Photonic Structures for Fluorescent Concentrators with Increased Efficiencies
J. C. Goldschmidt, M. Peters, L. Prönneke, L. Steidl, R. Zentel, B. Bläsi, A. Gombert, S. Glunz, G. Willeke, and U. Rau,
phys. stat. solidi (a) **205**, 2811 (2008)

Electroluminescence Analysis of Cu(In,Ga)Se_2 Thin-Film Modules
A. Helbig, T. Kirchartz, R. Schaeffler, J. H. Werner, and U. Rau,
in Proc. 24th Europ. Photovolt. Solar Energy Conf. (WIP, Munich, 2009) in press

Quantitative Information of Electroluminescence Images
A. Helbig, T. Kirchartz, and U. Rau,
in *Proc. 23rd Europ. Photovolt. Solar Energy Conf.,* eds. D. Lincot, H. Ossenbrink, P. Helm (WIP, Munich, 2008) p. 426

Quantitative Evaluation of Electroluminescence Images
A. Helbig, T. Kirchartz, and U. Rau,
in *The First International Forum on Multidisciplinary Education and Research for Energy Science* (Tokyo Institute of Technology, Tokyo, 2008) p. 43

Advanced Photovoltaic Test Park in Egypt for Investigating the Performance of Different Module and Cell Technologies
M. Ibrahim, B. Zinßer, H. El-Sherif, E. Hamouda, G. Makrides, G. E. Georghiou, M. B. Schubert, and J. H. Werner,
in *Proc. 24th Symp. Photovoltaische Solarenergie* (OTTI, Bad Staffelstein, 2009) p. 318

Optical Fine Structure of Single Ordered GaAs Quantum Dots
S. Kiravittaya, R. Zapf-Gottwick, M. Benyoucef, A. Rastelli, and O. G. Schmidt,
Physica E **40**, 29 (2008)

Reciprocity Between Electroluminescence and Quantum Efficiency Used for the Characterization of Silicon Solar Cells
T. Kirchartz, A. Helbig, W. Reetz, M. Reuter, J. H. Werner, and U. Rau,
Prog. Photovolt.: Res. Appl. ***17**, 394 (2009)*

Note on the Interpretation of Electroluminescence Images Using Their Spectral Information
T. Kirchartz, A. Helbig, and U. Rau,
Solar Energy Materials and Solar Cells **92**, 1621 (2008), doi:10.1016/j.solmat.2008.07.013

Construction Process and Read-out Electronics of Amorphous Silicon Position Detectors for Multipoint Alignment Monitoring
C. Köhler, M. B. Schubert, B. Lutz, J. H. Werner, J. Alberdi, P. Arce, J. M. Barcala, E. Calvo, A. Ferrando, M. I. Josa, A. Molinero, J. Navarrete, J. C. Oller, C. Yuste, A.Calderón, M. G. Fernández, G. Gómez, F. J. González-Sánchez, C. Martínez-Rivero, F. Matorras, T. Rodrigo, M. Sobrón, I. Vila, and A. L. Virto,
Nuclear Instruments and Methods in Physics **A608**, 55 (2009), doi:10.1016/j.nima.2009.06.058

Detailed Balance Theory of Excitonic and Bulk Heterojunction Solar Cells
T. Kirchartz, J. Mattheis, and U. Rau,
Phys. Rev. B **78**, 235320 (2008), doi:10.1103/PhysRevB.78.235320

Influence of Precursor Layer Ablation on Laser Doping of Silicon
J. R. Köhler and S. J. Eisele,
Prog. Photovolt.: Res. Appl. **x**, xx (2009) in press

Characterizing GaInP/GaInAs/Ge Multijunction Solar Cells with Electroluminescence
T. Kirchartz, A. Helbig, M. Hermle, U. Rau, and A. W. Bett,
in *Proc. 23rd Europ. Photovolt. Solar Energy Conf.,* eds. D. Lincot, H. Ossenbrink, P. Helm (WIP, Munich, 2008) p. 86

Quantification of Light Trapping Using a Reciprocity Between Electroluminescent Emission and Photovoltaic Action in a Solar Cell
T. Kirchartz, A. Helbig, and U. Rau,
Mater. Res. Soc. Symp. Proc. Volume 1101E, KK01-04 (2008)

Internal Voltages in GaInP/GaInAs/Ge Multijunction Solar Cells Determined by Electroluminescence Measurements
T. Kirchartz, U. Rau, M. Hermle, A. W. Bett, A. Helbig, and J. H. Werner,
Appl. Phys. Lett. **92**, 123502 (2008), doi:10.1063/1.29031019

Laser Doped Selective Emitters yield 0.5% Efficiency Gain
J. R. Köhler, P. Grabitz, S. J. Eisele, T. C. Röder, and J. H. Werner,
in *Proc. 24th Europ. Photovolt. Solar Conf.* (WIP, Munich, 2009) in press

Advanced Solar Cell Front Grid Optimization
G. Kulushich, R. Zapf-Gottwick, M. Mühlbauer, V. X. Nguyen, and J. H. Werner,
in *Proc. 24th Europ. Photovolt. Solar Energy Conf.* (WIP, Munich, 2009) in press

Silicon Solar Cells With Texturization By Metal Assisted Chemical Etching
M. Lipinski and J. Cichoszewski,
in *Proc. 24th Europ. Photovolt. Solar Energy Conf.* (WIP, Munich, 2009) in press

Texturization By Metal-Assisted Chemical Etching For Silicon Solar Cells
M. Lipinski and J. Cichoszewski,
in *Proc. 23rd Europ. Photovolt. Solar Energy Conf.,* eds. D. Lincot, H. Ossenbrink, P. Helm (WIP, Munich, 2008) p. 1911

Outdoor Efficiency of Different Photovoltaic Systems Installed in Cyprus and Germany
G. Makrides, B. Zinßer, G. E. Georghiou, M. B. Schubert, and J. H. Werner,
in *Proc. 33rd Photovoltaic Specialists Conf.* (IEEE Publishing Service, Piscataway, NY, 2008) p. 6959

Temperature Behaviour of Different Photovoltaic Systems Installed in Cyprus and Germany
G. Makrides, B. Zinßer, G. E. Georghiou, M. Schubert, and J. H. Werner,
Solar Energy Materials and Solar Cells **93**, 1095 (2009),
doi:10.1016/j.solmat.2008.12.024

Two Year Performance Evaluation of Different Grid Connected Photovoltaic Systems
G. Makrides, B. Zinßer, G. E. Georghiou, M. B. Schubert, and J. H. Werner,
in *Proc. 34th IEEE Photovoltaic Specialists Conf.* (IEEE Publishing Service, Piscataway, NY, 2009) in press

Error Sources in Outdoor Performance Evaluation of Photovoltaic Systems
G. Makrides, B. Zinßer, M. Norton, G. E. Georghiou, M. B. Schubert, and J. H. Werner,
in *Proc. 24th Europ. Photovolt. Solar Energy Conf.* (WIP, Munich, 2009) in press

Potential of Photovoltaic Systems in Countries with High Solar Irradiation
G. Makrides, B. Zinßer, M. Norton, G. E. Georghiou, M. B. Schubert, and J. H. Werner,
in *Renewable and Sustainable Energy Reviews* **756**, xx (2009) in press, doi:10.1016/j.rser.2009.07.021

Finite Mobility Effects on the Radiative Efficiency Limit of pn-Junction Solar Cells
J. Mattheis, J. H. Werner, and U. Rau,
Phys. Rev. B **77**, 270 (2008)

In-Situ Series Connection for Thin Film Photovoltaic Modules
R. Merz, J. H. Werner, and M. B. Schubert,
in *The First International Forum on Multidisciplinary Education and Research for Energy Science* (Tokyo Institute of Technology, Tokyo, 2008) p. 99

In-Situ Series Connection for Thin Film Photovoltaic Modules
R. Merz, M. M. Adachi, M. B. Schubert, and J. H. Werner,
in *Proc. 23rd Europ. Photovolt. Solar Energy Conf.*, eds: D. Lincot, H. Ossenbrink, P. Helm (WIP, Munich, 2008) 2411

Flexible PV Modules by Monolithic Series Connection During Thin Film Deposition
R. Merz, M. B. Schubert, and J. H. Werner,
Photovoltaics World **1**, 50 (2009)

Novel In Situ Series Connection for Thin Film Photovoltaic Modules
R. Merz, J. Kistner, M. B. Schubert, and J. H. Werner,
in *Thin Film Solar Technology*, edited by A. E. Delahoy and L. A. Eldada, (Proc. SPIE **7409**, San Diego, 2009) 74090K, doi:10.1117/12.826132

Optimization of the In Situ Series Connection of Amorphous Silicon Solar Modules on Glass and Foil Substrates
R. Merz, J. Kistner, M. A. Bouattour, and M. B. Schubert,
physica status solidi (c) **x**, xx, (2009) in press

In Situ Series Connection for Multi-junction Thin Film Cells
R. Merz, J. Kistner, and M. B. Schubert,
in *Proc. 24th Europ. Photovolt. Solar Energy Conf.* (WIP, Munich, 2009) in press

String-based Maximum Power Tracking of Photovoltaic Systems
R. Merz, A. S. Garamoun, T. Wurster, J. Jochen, and M. B. Schubert,
in *Proc. 24th Europ. Photovolt. Solar Energy Conf.* (*WIP, Munich, 2009*), in press

Improving Screen Printed Front Contacts by Predrying
M. Mühlbauer, V. X. Nguyen, and R. Zapf-Gottwick,
in *Proc. 24th Europ. Photovolt. Solar Energy Conf.* (WIP, Munich, 2009) in press

Analysis of Screen Printed Solar Cell Emitters
V. X. Nguyen, M. Reuter, P. Gedeon, and R. Zapf-Gottwick,
in *Proc. 24th Europ. Photovolt. Solar Energy Conf.* (WIP, Munich, 2009) in press

Design of Photonic Structures for the Enhancement of the Light Guiding Efficiency of Fluorescent Concentrators
M. Peters, J. C. Goldschmidt, P. Löper, L. Prönneke, B. Bläsi, and A. Gombert,
in *Photonics for Solar Energy Systems II*, edited by A. Gombert, (Proc. SPIE **7002**, Strasbourg, 2008) 70020V, doi:10.1117/12.781087

Measurement and Simulation of Enhanced Photovoltaic System with Fluorescent Collectors
L. Prönneke, G. Glaeser, Y. Uslu, and U. Rau,
in *Proc. 24th Europ. Photovolt. Solar Energy Conf.* (WIP, Munich, 2009) in press

Loss Mechanisms in Photovoltaic Fluorescent Collectors
L. Prönneke and U. Rau,
Mater. Res. Soc. Symp. Proc. *1101,* KK08-04 (2008)

Geometry Effects on Photon Collection in Photovoltaic Fluorescent Collectors
L. Prönneke and U. Rau,
in *Photonics for Solar Energy Systems II*, edited by A. Gombert, (Proc. SPIE **7002**, Strasbourg, 2008) 70020U, doi:10.1117/12.780954

Non-radiative Recombination in Photovoltaic Fluorescent Collectors
L. Prönneke, J. C. Goldschmidt, M. Peters, and U. Rau,
in *The First International Forum on Multidisciplinary Education and Research for Energy Science* (Tokyo Institute of Technology, Tokyo, 2008), p. 49

Electroluminescence Imaging of $Cu(In,Ga)Se_2$ Thin Film Solar Modules
U. Rau, T. Kirchartz, A. Helbig, and B. E. Pieters,
Mat. Res. Soc. Symp. Proc. **1165**, M03 (2009)

50 µm Thin Solar Cells with 17.0 % Efficiency
M. Reuter, W. Brendle, O. Tobail, and J. H. Werner,
Solar Energy Materials and Solar Cells **93**, 704 (2008)

0.4% Absolute Efficiency Gain of Industrial Solar Cells by Laser Doped Selective Emitter
T. Röder, P. Grabitz, S. J. Eisele, C. Carlsson, J. R. Köhler, and J. H. Werner,
in *Proc. 34th Photovoltaic Specialists Conf.* (IEEE Publishing Service, Piscataway, NY, 2009) in press

Fill Factor Loss of Laser Doped Textured Silicon Solar Cells
T. Röder, A. Esturo-Bretón, S. Eisele, C. Carlsson, J. R. Köhler, and J. H. Werner,
in *Proc. 23rd Europ. Photovolt. Solar Energy Conf.*, eds: D. Lincot, H. Ossenbrink, P. Helm (WIP, Munich, 2008) p. 1740

Laser Doped Selective Emitter for Silicon Solar Cells
T. Röder, C. Carlsson, J. R. Köhler, and J. H. Werner,
in *The First International Forum on Multidisciplinary Education and Research for Energy Science* (Tokyo Institute of Technology, Tokyo, 2008) p. 17

Amorphous Silicon Based p–i–i–n Photodetector Detects 12 nm Thin Protein Layers
M. Sämann, L. Steinle, and M. B. Schubert,
J. Non-Cryst. Solids **354**, 2575 (2008)

Amorphous Silicon Based p-i-i-n Photo Detectors for Point-of-Care Testing
M. Sämann, D. Furin, J. Thielmann, A. Pfäfflin, G. Proll, C. Harendt, G. Gauglitz, E. Schleicher, and M. B. Schubert,
physica status solidi (c) x, xx, (2009) in press

Characterization of Sputtered and Laser Recrystallized Phosphorus Doped ZnO Thin Films

M. Sämann, S. J. Eisele, and G. Bilger,
in *Proc. ALC´09,* (Maui, Hawaii, 2009) in press

Flexible Solar Cells and Modules
M. B. Schubert and R. Merz,
Phil. Mag. **89**, 2623 (2009), doi:10.1080/14786430903147122

Thin Film on CMOS Active Pixel Sensor for Space Applications
J.-D. Schulze Spüntrup, J. N. Burghartz, H.-G. Graf, C. Harendt,
F. Hutter, M. Nicke, U. Schmidt, M. Schubert, and J. Sterzel,
Sensors **8**, 6340 (2008), doi:10.3390/s8106340

Energy Yield Forecasting for High-Efficiency PV Systems in Three Locations Using Artificial Neural Networks
M. B. Strobel, B. Zinßer, G. Makrides, M. Norton, T. R. Betts,
G. E. Georghiou, M. Schubert, and R. Gottschalg,
in *Proc. 24th Europ. Photovolt. Solar Energy Conf.* (WIP, Munich, 2009) in press

Lateral Homogeneity of Porous Silicon for Large Area Transfer Solar Cells
O. Tobail, Z. Yan, M. Reuter, and J. H. Werner,
Thin Solid Films **516**, 6959 (2008)

Novel Separation Process for Free-Standing Silicon Thin-Films
O. Tobail, M. Reuter, and J. H. Werner,
Solar Energy Materials and Solar Cells **93**, 710 (2009)

Directional Selectivity and Light-Trapping in Solar Cells
C. T. Ulbrich, S. Fahr, M. Peters, J. Üpping, T. Kirchartz, C. Rockstuhl, J. C. Goldschmidt, P. Löper, R. Wehrspohn, A. Gombert, F. Lederer, and U. Rau,
Proc. SPIE **7002**, 70020A (2008) , doi:10.1117/12.781248

Directional Selevtivity and Ultra-Light-Trapping in Solar Cells
C. T. Ulbrich, S. Fahr, J. Üpping, M. Peters, T. Kirchartz, C. Rockstuhl, R. Wehrspohn, A. Gombert, F. Lederer, and U. Rau,

in *The First International Forum on Multidisciplinary Education and Research for Energy Science* (Tokyo Institute of Technology, Tokyo, 2008) p. 15

Directional Selectivity and Ultra-Light-Trapping in Solar Cells
C. T. Ulbrich, S. Fahr, J. Üpping, M. Peters, T. Kirchartz, C. Rockstuhl, R. Wehrspohn, A. Gombert, F. Lederer, and U. Rau,
phys. stat. solidi (a) **205**, 2831 (2008) , doi:10.1002/pssa.200880457

Enhanced Light-trapping in Solar Cells by Directional Selective Optical Filters
C. T. Ulbrich, T. Kirchartz, and U. Rau,
Mater. Res. Soc. Symp. Proc. **1101E,** KK08-03 (2008)

Improved Concept for Industrial Screen Printing Line
R. Zapf-Gottwick, J. Cichoszewski, O. Fechtig, M. Mühlbauer, K. Metzner, T. Schlenker, D. Manz, and J. H. Werner,
in *Proc. 24th Europ. Photovolt. Solar Energy Conf.* (WIP, Munich, 2009) in press

New Industrial Screen Printing Line for Silicon Solar Cells
R. Zapf-Gottwick, J. Cichoszewski, O. Fechtig, M. Mühlbauer, J. H. Werner, D. Manz, K. Metzner, and T. Schlenker,
in *The First International Forum on Multidisciplinary Education and Research for Energy Science* (Tokyo Institute of Technology, Tokyo, 2008) p. 9

Temperature and Intensity Dependence of Twelve Photovoltaic Technologies
B. Zinßer, G. Makrides, M. B. Schubert, G. Georghiou, and J. H. Werner,
in *Proc. 23rd Europ. Photovolt. Solar Energy Conf.*, eds. D. Lincot, H. Ossenbrink, P. Helm (WIP, Munich, 2008) p. 3249

Jahresenergieertrag von 13 verschiedenen Photovoltaik-Technologien in Deutschland und Zypern
B. Zinßer, G. Makrides, M. B. Schubert, G. E. Georghiou, and J. H. Werner,
in *Proc. 23rd Symp. Photovoltaische Solarenergie*, (OTTI, Bad Staffelstein, 2008) p. 294

Temperature and Irradiance Effects on Outdoor Field Performance
B. Zinßer, G. Makrides, M. B. Schubert, G. E. Georghiou, and J. H. Werner,
in *Proc. 24th Europ. Photovolt. Solar Energy Conf.* (WIP, Munich, 2009) in press

Mehrertrag durch Nachführung in Deutschland, Zypern und Ägypten
B. Zinßer, G. Makrides, M. Ibrahim, H. El-Sherif, E. Hamouda, G. E. Georghiou, M. B. Schubert, and J. H. Werner,
in *Proc. 24th Symp. Photovoltaische Solarenergie* (OTTI, Bad Staffelstein, 2009) p. 312

Das *ipe* ist Mitglied im PV-UNI-NETZ

PV-UNI-NETZ ist ein Verbund unabhängiger Hochschulprofessoren, die Photovoltaik in Forschung, Entwicklung und Lehre betreiben.

PV-UNI-NETZ ist Forum für die Diskussion und Koordination neuer Ideen und zukunftsweisender Photovoltaikforschung an deutschen Universitäten und universitätsnahen Instituten.

PV-UNI-NETZ vertritt die Interessen und das Wissen der deutschen Universitäten im Bereich der Photovoltaik.

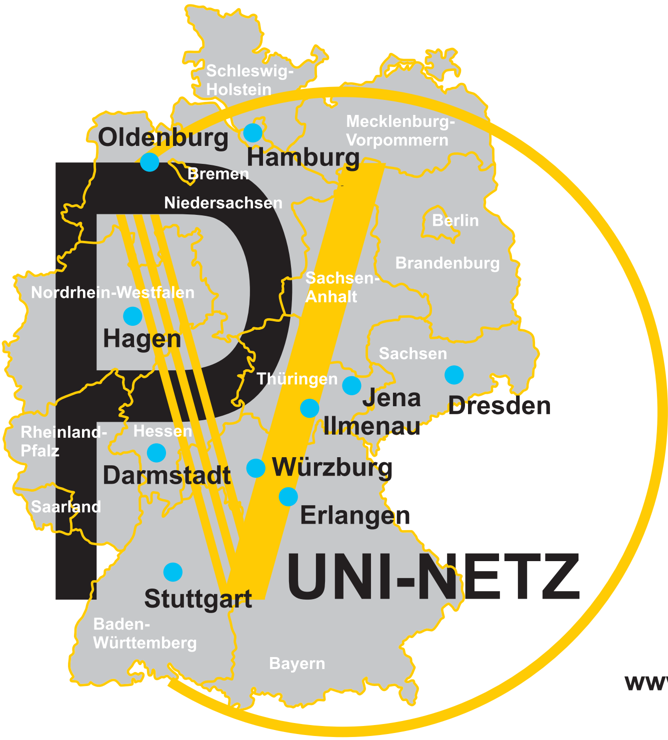

www.pv-uni-netz.de

Lehrveranstaltungen
Lectures

Promotionen
Ph. D. Theses

Diplomarbeiten
Diploma Theses

Studienarbeiten
Major Term Projects

Gäste & ausländische Stipendiaten
Guests

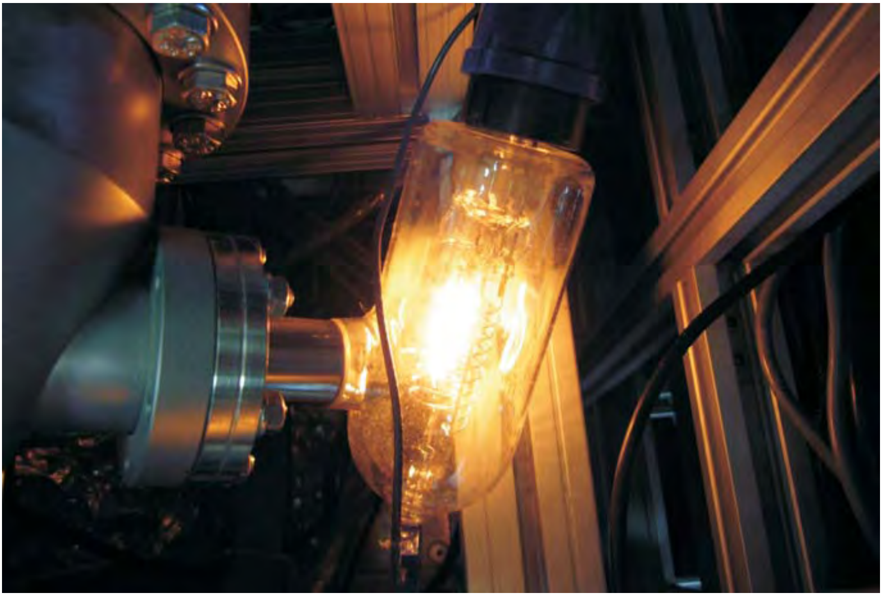

Bauelemente der Mikroelektronik (1. Semester)
J. H. Werner

Energiebänder und Leitfähigkeit
Silicium - der Werkstoff der Mikroelektronik
Elektronen und Löcher in Halbleitern
Ströme in Halbleitern
Nichtgleichgewicht und Injektion
Elektrostatik des pn-Übergangs
Ströme im pn-Übergang

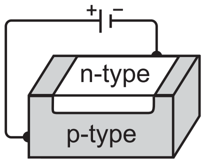

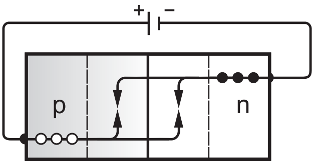

Energiewandlung (6. / 8. Semester)
J. H. Werner

Grundlagen der Kernenergie
Thermodynamik
Direkte Nutzung der Sonnenenergie (Solarthermie, Photovoltaik)
Indirekte Nutzung der Sonnenenergie (Wasserkraft, Windenergie)
Chemische Wandlung und Speicherung elektrischer Energie

Laser and Light Sources (5. / 7. Semester)
J. R. Köhler

The Human Eye
Light and Color
Photometry
Incoherent Light Sources
Light Emitting Diodes
Lasers
Laser Processing

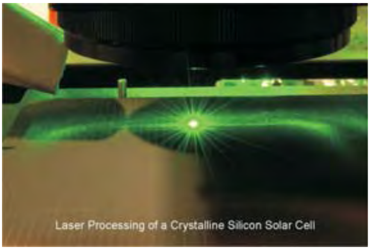

Optoelectronic Devices and Circuits I (6. / 8. Semester)
J. H. Werner

Basic physics
Thermal radiation
Coherence
Semiconductor basics
Excitation and recombination processes in semiconductors
Light emitting diodes
Semiconductor lasers
Glass fibers
Photodetectors

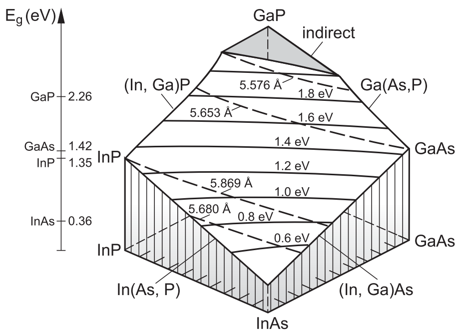

Photovoltaics (6. / 8. Semester)
J. H. Werner

Energy data
The solar spectrum
Potential of solar radiation
The principal function of photovoltaic systems
Generation and recombination in semiconductors
Basic semiconductor equations
pn-Junctions
Current/voltage-curve of solar cells
Maximum efficiency of solar cells
Preparation of crystalline silicon
Amorphous silicon solar cells
$Cu(In,Ga)Se_2$ solar cells
Technology of crystalline
silicon solar cells

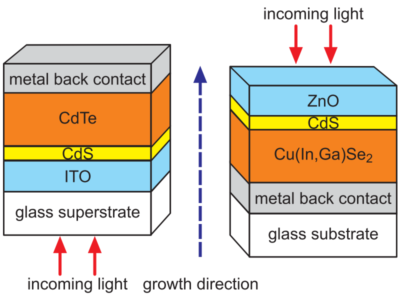

Solid State Electronics (5. / 7. Semester)
J. H. Werner

Free electrons as particles and waves
Electronic bands in solids
Band diagrams of semiconductors
Currents in semiconductors
Emission of electrons from metals and semiconductors
The Schottky-contact
Photoeffects in semiconductors

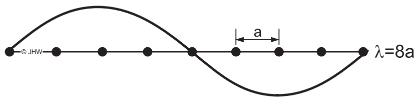

Wissenschaftliches Vortragen und Schreiben I (6. Semester)
J. H. Werner

Kernbotschaften
Aufbau eines Vortrags
Standardfehler (Strukturfehler, Technikfehler, Fehler im Auftreten)
Praktische Schritte zum Vortrag
Selbst- und Fremdbeurteilung (mit Videoaufzeichung)

Wissenschaftliches Vortragen und Schreiben II (7. Semester)
J. H. Werner

Kernbotschaften
Aufbau und Elemente einer Publikation
Bilder, Tabellen und Referenzen

Praktische Übungen im Labor „Halbleitermesstechnik" (7. Semester)
M. B. Schubert

Herstellverfahren von Halbleitern und dünnen Schichten
elektrische Messtechniken für Minoritäten und Majoritäten
optische Messtechnik
strukturelle Messtechniken

Promotionen
Ph. D. Theses

Julian Mattheis
Mobility and Homogeneity Effects on the Power Conversion Efficiency of Solar Cells

Johannes Philipp Rostan
a-Si:H/c-Si Heterojunction Front- and Back Contacts for Silicon Solar Cells with P-type Base

Osama Tobail
Porous Silicon for Thin Solar Cell Fabrication

Diplomarbeiten
Diploma Theses / Master Theses

Ali Bouattour
Direct X-Ray Detection for Medical Imaging Applications

Ivan Dinev
Entwicklung u. Aufbau eines Solarsystems mit elektronischer Verschaltung von Solarmodulen mit MPP-Tracking

Matthias Feinäugle
Phosphorus-doped Amorphous Silicon Nitride Films Applied to Crystalline Silicon Solar Cells

Fabian Fertig
Shunt Detection in Crystalline Silicon Solar Cells using IR Thermography

Panagiotis Gedeon
Lebensdaueruntersuchung an c-Si Wafern

Jaime González
Laser Edge Isolation for Silicon Solar Cells

Daniel Hammer
Photoinduzierte Oberflächenoxidation von kristallinem Silizium

Erik Hoffman
Laserinduzierte Vorderseitenmetallisierung auf c-Silizium Solarzellen

Markus Hofmann
Optimierung der Prozessparameter der Laserdotierung mit Hilfe der statistischen Versuchsplanung

Jens Kistner
Photoluminescence of Nanocrystalline Silicon – Theory and Experiment

Stefan Klingbeil
Diffusion durch poröses Silizium für einstufige selektive Emitter

Boris Misic
Outdoor Measurement of the Current-Voltage Characteristics of Photovoltaic Modules

Pongstorn Ngamskulrungroj
Charakterisierung und Analyse des Emitters von String-Ribbon Solarzellen

Mustafa Sarpasan
Prozessansteuerung für die Laserbearbeitung von Silizium

Max Siegloch
Kennlinienbasierte Abschattungsanalyse bei photovoltaischen Systemen

Weng Song
Quantenausbeute an großen Solarzellen

Yusuf Uslu
Diffusion und Reaktionen in metallischen Vorläuferschichten von CIGS-Solarzellen

Studienarbeiten
Major Term Projects

Christian Banzhaf
Rückseitenoptimierung von Si-Solarzellen

Kai Carstens
Laserunterstützte Oberflächentexturierung von kristallinem Silizium

Morris Dahlinger
Herstellung und Charakterisierung von Bordotierschichten für die Laserdotierung

Liangdong Du
Entwicklung von aluminiumdotierten Zinkoxidschichten für Photodioden und Solarzellen auf flexiblen Substraten

Dimitar Ganchev
Beleuchtungsabhängige Vermessung von Solarmodulen

Panagiotis Gedeon
Analoges Maximum-Power-Point-Tracking für Solarmodule

Haithem Gribaa
Optische Optimierung von Solarzellen durch streuende Kontaktbänder

Heike Isemann
Characterization of Amorphous Silicon Phototransistors and Pixels for Digital Imaging Applications

Bodo Konrad
Solarzellencharakterisierung mittels Elektrolumineszenz

Peter Kozlowski
Charakterisierung und Optimierung von Einzelschichten für Silizium-Dünnschicht-Solarzellen

Mariam Nader
Characterization and Electrical Loss Analysis for Screen-printed Multicrystalline Silicon Solar Cells at *ipe*

Neli Ovcharova
Ansteuerung und Auswertung am Sonnensimulator

Andreas Schirmer
Analyse und Charakterisierung von String-Ribbon Solarzellen

Mohamed Shalaby
Analyzing Solar Cells Using Simulation Software (INSEL & KIVAP)

Yusuf Uslu
Physikalische Gasphasenabscheidung von SiO_2, Si_3N_4 zur Herstellung energie- und winkelselektiver Strukturen

Claus Villringer
Simulation von zwei verschiedenen Solarzellentypen in Trogsystemen

Dongdao Zhang
Low Temperature Front Side Metallization on Silicon by Using Polymer Paste

Song Yang
Messplatzaufbau zur beleuchtungsabhängigen Charakterisierung von amorphem Silizium

Thomas Wurster
Effizienzsteigerung der elektronischen Verschaltung von Solarmodulen

Gäste & ausländische Stipendiaten
Guests

Michael Adachi
University of Waterloo, Waterloo, Ontario, Kanada

Pedro Alpuim
Universidade do Minho, Guimarães, Portugal

Enkhbajar Batzorig
Mongolian University of Science and Technology,
Ulaanbaatar, Mongolei

Amr Bayoumi
German University in Cairo, Ägypten

Li Da
Tongji University , Shanghai, China

Ahmed Samir Garamoun
Benha High Institute of Technology, Cairo, Ägypten

Jaime Gonzáles
Universidad Politécnica de Madrid, Spanien

Reem Mansour
German University in Cairo, Ägypten

José Rivera
Panama Technological University, Panama, Panama

Toshiyuki Sameshima
Tokyo University of Agriculture and Technology, Tokyo, Japan

Salma Shabayek
Arabic Academy for Science and Technology, Alexandria, Ägypten

Mohamed Shalaby
German University in Cairo, Ägypten

Danilo Tebaldi
Instituto Nacional de Telecomunicações (Inatel), Santa Rita do Sapucaí, Minas Gerais, Brasilien

Mariam Nader Yacoub
German University in Cairo, Ägypten

Shinya Yoshidomi
Tokyo University of Agriculture and Technology, Tokyo, Japan

Was sonst noch war ...
More than Science ...

Mitarbeiterliste
Staff Members

Lageplan
Location Map

Was sonst noch war ...
More than Science ...

ipe 2.0

Damit die Protoypen der industriellen Siebdruckanlagen Anfang 2008 einen Weg in unser Labor fanden, brauchte das *ipe* erst ein großes Loch in der Laborwand, dann eine neue große Türe, dazu natürlich noch ein paar Umbauten an Lüftung, Wasser- und Medienleitungen, einen Kompressor für die Kühlung. Ein paar Wände und Decken mussten auch noch weg. Spezialisten für solche Wünsche finden wir im Dezernat VI - Technik und Bauten, im Universitätsbauamt und natürlich auch beim allzeit hilfreichen Gebäudemanagement. Ohne das Engagement und die Kreativität dieser Kolleginnen und Kollegen im Umgang mit den viel zu knappen Ressourcen hätten wir keine Chance, neue Forschungsgebiete zu eröffnen. Mit ihrer Unterstützung konnten wir aber 2009 gleich noch eine neue Mehrkammeranlage zur Plasmaabscheidung von Siliziumdünnschichten in Betrieb nehmen, dieses Mal mit Portalkran, neuer 100 A-Leitung und Gasversorgung. Was 2010 kommt, verrät erst der nächste Jahresbericht!

ipe 2.0

The prototypes of industrial screen printing machines found their way into the *ipe* laboratories via a big hole in the facade which was then closed by a new big door. Furthermore, the screen printing equipment needed some rearrangements and extensions of venting, water and media supply, and special cooling. Some walls and ceilings had to disappear as well. We find real specialists for working through such a wish list at the Central Department VI (Technology and Buildings) of the Universität Stuttgart, at the Universitätsbauamt and at the always very supportive Technical Facility Management. Without the commitment of those colleagues, and their creativity in managing the very limited resources, we would have no chance at all of opening new research areas. Relying on their support, however, we could start operation of a new cluster tool deposition system for thin silicon films in 2009, this time including a gantry crane, new 100 A electricity supply and additional gas lines.

ipe-Ausflug

Man spricht so schnell von „Highlights"…, unser Ausflug 2008 verdient aber wirklich diesen Titel! Kanufahren in Fischingen bei Horb; ganz trocken ist keiner geblieben. Und dann die einmalige Gelegenheit, bei Rottweil einen Tandemflug mit dem Gleitschirm zu machen. Besonders kribbelig war die Tatsache, dass die Flüge mit der Seilwinde gestartet wurden! Diesmal war Essen und Trinken absolut zweitrangig.

Energiewandlung - live

Zuerst die Theorie, dann die Praxis. Unsere Studierenden durften ihrer Kreativität freien Lauf lassen: Aus Resten und Abfällen wurden wieder funktionierende Energiewandler gebaut.

ETI-Cup

Nach einjähriger Abstinenz haben wir den ETI-Cup wieder nach Hause geholt. Nach einem ausgeglichenen Endspiel, dem es an nennenswerten Höhepunkten und Toren mangelte, waren ein überragender Torwart und treffsichere Schützen im 9-Meter-Schießen der Schlüssel zum verdienten ETI-Cup-Sieg. Die Trophäe bleibt ein Jahr bei uns!

ipe-Getaway

Everybody talks about "highlights"… Our getaway 2008 was one! We went for canoeing; no chance not to get wet. The big opportunity was to try a tandem flight with the parawing! Eating and drinking were secondary this time.

Energy Conversion - here and now

Ideas have been put into practice. Our students could test the theory taught during the lecture "Energy Conversion". Yes, they were able to make up functional models out of remains and waste as material.

ETI Cup

We made it again! The very sought-after ETI cup is in our hands again! Looking for the reason? Just ask our strongly motivated, well-trained and international *ipe* soccer team!

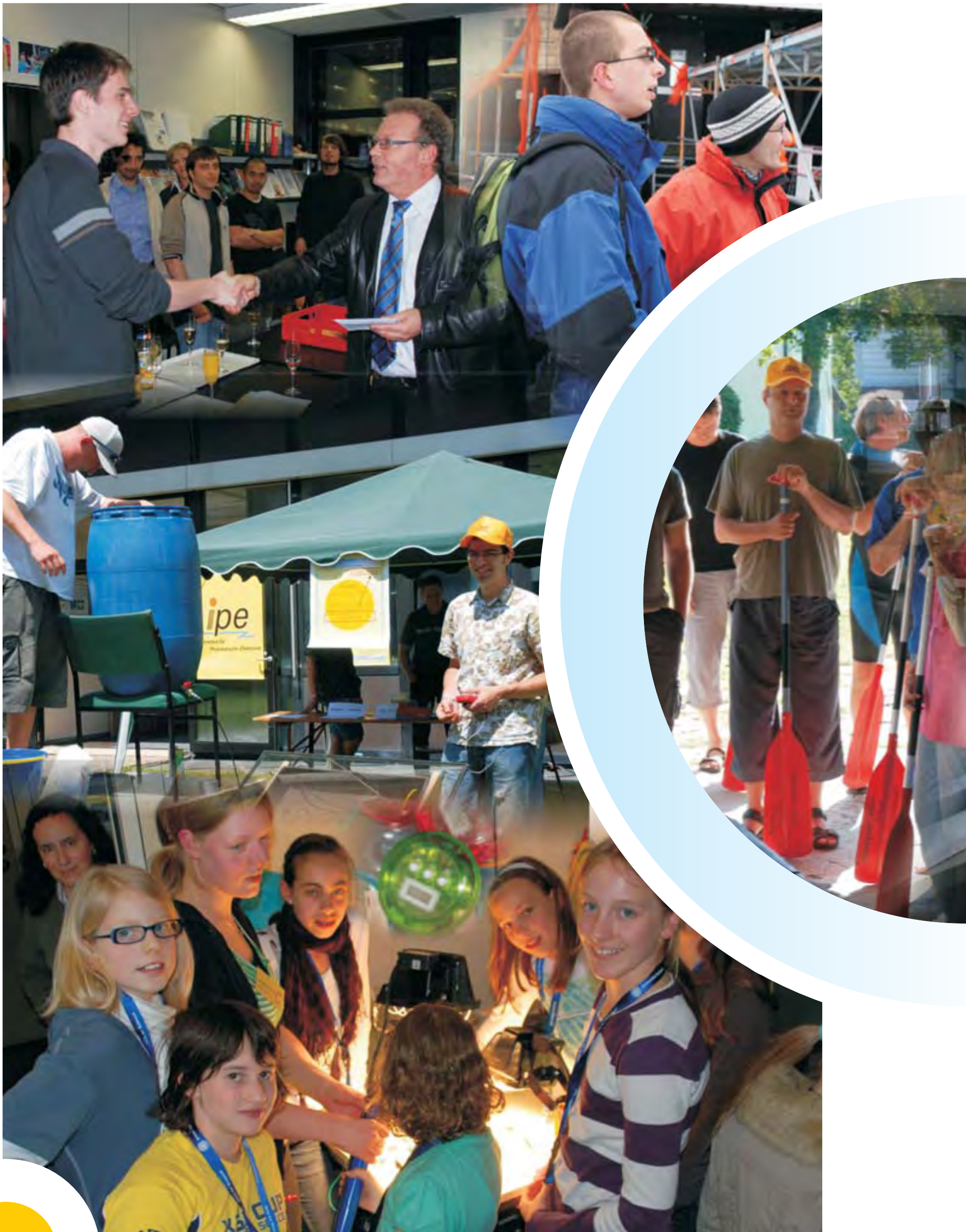
ipe

Girls' Day

Das Motto war wieder einmal „Lass die Mädchen ran”! Keine Angst vor naturwissenschaftlich-orientierten Studienfächern! So freute sich das *ipe* über regen Besuch einer Mädchengruppe, die unter der fachkundigen Anleitung von Liv, Anke und Rainer erste Löterfahrungen machte und Fragen zu allem „Photovoltaischen” stellen konnte.

Jahresabschlussfeier

Das Besondere an der Feier 2008 war, dass gute Studierende zum Zuge kamen. Für gute Leistungen im Sommersemester gab es Ermunterung und ein kleines Geschenk. Wie immer war das Büffet lecker, und die Jungs (!) haben sich lustige Spiele einfallen lassen.

Herzlichen Glückwunsch!

Markus Schubert hat es geschafft: 25 Jahre Universitätsdienst sind vollbracht! Wir alle am *ipe* gratulieren ganz herzlich und hoffen, dass noch viele kreative Jahre dazu kommen.

Girls' Day

Once again the motto: let the girls do it! No fear of scientific-technical subjects. The *ipe* was happy to welcome a highly motivated group of high school girls during the University's “Girl's Day”. Thank you, Liv, Anke and Rainer, for your commitment!

At the end of 2008

Excellent students were praised at our end-of-year celebration 2008; they received a small gift. Our buffet was tasty, as usual, and our PhD students again had good gaming ideas (teasing JHW)!

Congratulations Markus!

Markus Schubert made it: he celebrated his 25th anniversary at the university! The *ipe* staff says “Congratulations”!

Mitarbeiterliste

Staff Members

Titel / Name	Telefon 0711 - 685 - ...	E-Mail (vorname.name) @ipe.uni-suttgart.de	Arbeitsgebiet
Leo Bauer	60105	leo.bauer	Metallisierung, Photo-arbeiten, Maskentechnik
Dr.-Ing. Gerhard Bilger	67176	gerhard.bilger	Oberflächenanalytik; Technologie Support
Dipl.-Ing. Mohamed Ali Bouattour	67181	ali.bouattour	Integrierte Photovoltaik
Dipl.-Ing. Jakub Cichoszewski	69219	jakub.cichoszewski	Texturen für Solarzellen
Dipl.-Ing. Christian Ehling	67161	christian.ehling	Amorphe Passivierschichten
Dipl.-Ing. Sebastian Eisele	67198	sebastian.eisele	Laserdotieren
Dr.-Ing. Gerda Gläser	69214	gerda.glaeser	Charakterisierung von Solarzellen
Dipl.-Nat. Anke Helbig	67169	anke.helbig	Lumineszenz
Irmgard Kerschbaum	67158	irmgard.kerschbaum	Buchhaltung

Lic. Phil. Isabel Kessler	67141	isabel.kessler	Sekretariat, Verwaltung
Dipl.-Ing. Jens Kistner	69223	jens.kistner	amorphe Solarzellen, Lumineszenz
Dipl.-Phys. Christiane Köhler	67182	christiane.koehler	Leitung Technologiesupport, Niedertemperaturtechnologie
Dr.-Ing. Jürgen Köhler	67159	juergen.koehler	Laserprozesse, Verwaltung
M. Sc. Gordana Kulušič	69218	gordana.kulusic	Siebdruckprozesse, Modellierung
M. Sc. Da Li	67171	da.li	Charakterisierung
Brigitte Lutz	67200	brigitte.lutz	Analytik, Elektrochemie
Rainer Maak	67158	rainer.maak	Buchhaltung
Dipl.-Ing. Rainer Merz	67184	rainer.merz	Integrierte Photovoltaik
Heike Mohr	67141	heike.mohr	Sekretariat, Verwaltung
Dr.-Ing. Maria Mühlbauer	67179	maria.muehlbauer	Siebdruckprozesse, Baseline

M. Sc. Viet Xuan Nguyen	67160	viet.nguyen	Siebdruckprozesse, Diffusionen
Dipl.-Phys. Liv Prönneke	67180	liv.proenneke	Optik von Solarzellen
Dipl.-Ing. Michael Reuter	67168	michael.reuter	Dünnes kristallines Silizium
Anton Riß	67214	anton.riss	Werkstatt
Dipl.-Phys. Tobias Röder	69213	tobias.roeder	Laserprozesse
Dipl.-Ing. Marc Sämann	67142	marc.saemann	Amorphes Silizium, Biosensoren, Administrator
Dr.-Ing. Markus Schubert	67145	markus.schubert	Stellv. Institutsleiter, amorphes und nanokristallines Si
Prof. Dr. Dr. habil. Jürgen H. Werner	67140	juergen.werner	Institutsleiter, Leitung Forschung, Lehre, Verwaltung
Dipl.-Ing. (FH) Birgitt Winter	67162	birgitt.winter	Technologie kristalliner Si-Solarzellen
Dr. rer. nat. Renate Zapf-Gottwick	69225	renate.zapf-gottwick	Industrielle Solarzellen
Dipl.-Ing. Bastian Zinßer	67170	bastian.zinsser	Erträge PV-Anlagen

Lageplan
Location Plan

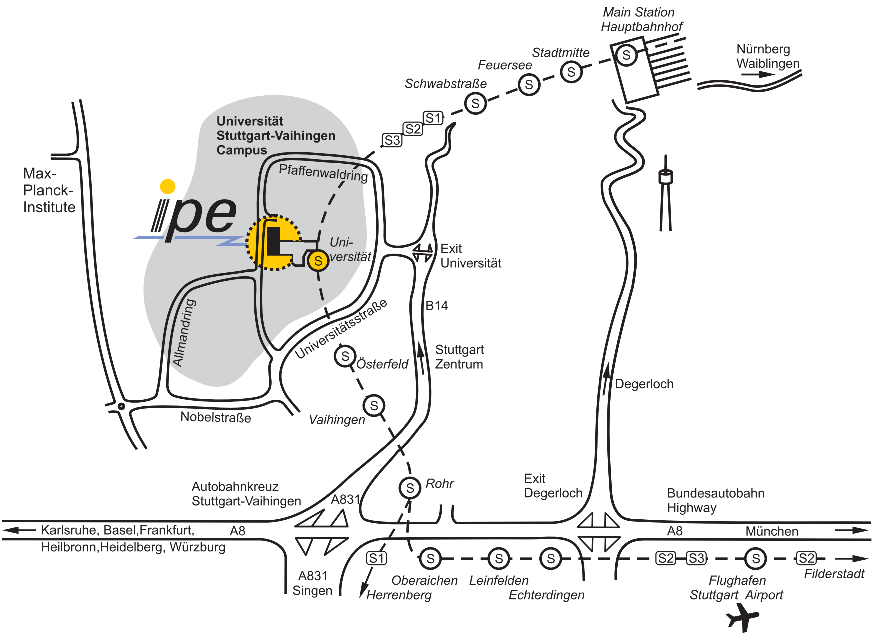

ipe

Institut für Physikalische Elektronik
Pfaffenwaldring 47
70569 Stuttgart

Tel.: 0711 / 685-67141

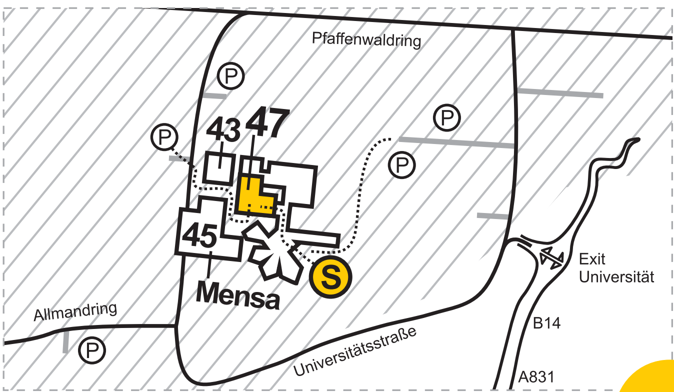

Institut für Physikalische Elektronik
Universität Stuttgart

Pfaffenwaldring 47
70569 Stuttgart

Phone: +49 711 685 67141
FAX: +49 711 685 67143

www.ipe.uni-stuttgart.de